Russian Chemical Reviews **82** (5) 429 – 448 (2013) © 2013 Russian Academy of Sciences and Turpion Ltd

DOI 10.1070/RC2013v082n05ABEH004337

Colloidal quantum dots in solar cells

L M Nikolenko, V F Razumov

Contents

I.	Introduction	429
II.	Parameters determining the efficiency of solar energy conversion	431
III.	Synthesis of colloidal quantum dots	432
IV.	Charge transport properties of layers of quantum dots. Surface modification of quantum dots	433
V.	Multiple exciton generation and the role of 'hot' charge carriers in quantum dots	433
VI.	Schottky-junction solar cells	434
VII.	Hybrid quantum dots/conjugated polymer heterojunction solar cells	436
VIII.	Semiconductor/semiconductor heterojunction solar cells	440
IX.	Quantum dot-sensitized solar cells	442
X.	Conclusion	444

Abstract. Published data on the use of colloidal quantum dots in solar cells are analyzed and generalized. Various types of solar cells, their design and principles of operation are considered. The key factors influencing parameters of these devices are discussed. The bibliography includes 184 references.

I. Introduction

Conversion of solar energy to electricity is a promising avenue in green power engineering. Presently, first-generation devices based on crystalline silicon still dominate among various types of solar cells†. They have been known for more than five decades. The operating efficiency of such devices is characterized by the energy conversion coeffcient (η) whose best value is as high as about 25%,[1] being close to the theoretical limit for single-junction solar cells (31%).[2] The operating life of the first-generation solar cells is more than 25 years. However, they are expensive due to strict requirements on the purity of the material and to very complicated fabrication process. Second-generation solar cells are based on amorphous or polycrystalline silicon. They are cheaper owing to cheaper fabrication technologies but less efficient.

Third-generation solar cells have various designs resulting from different technologies; a particular case is the use of nanostructures as solar cell components. Energy produced by the third-generation solar converters is much cheaper than that produced by older-generation solar cells. For instance, organic solar cells represent an attractive and, which is more important, cheap alternaive to silicon cells. It is believed that the cost of 1 kW h produced by organic solar cells can be as low as 1 – 2 US cent.[3] Frequently used working materials for this type of solar cells include mixtures of fullerene derivatives (electron-accepting materials) and novel polymers (electron-donating materials).[4 – 8] These components are well soluble in organic solvents, which makes it possible to deposit them on flexible polymeric substrates using printing technique. The technology which utilizes soluble organic semiconductor materials allows one to produce liquid 'ink'. It has been well developed and is used by many companies. The appropriateness of using organic solar cells is governed by a combination of three factors, namely, the prime cost, operating life and efficiency. Modern polymer – fullerene solar cells are characterized by reasonably high efficiency of solar energy conversion (up to $\sim$10%).[9 – 11]

Another type of third-generation solar cells, Grätzel photochemical cells based on nanostructured TiO_2 or ZnO layers covered with a sensitizing dye, is also characterized by high solar energy conversion efficiency (η_{max} = 12%).[12]

This review concerns yet another promising avenue in modern photovoltaics, namely, the use of semiconductor nanocrystals or quantum dots (QDs) prepared by methods of colloidal synthesis. Quantum dots exhibit unique optical and electronic properties and can be readily incorporated into liquid-phase technologies for fabrication of solar cells,

L M Nikolenko, V F Razumov Institute of Problems of Chemical Physics, Russian Academy of Sciences, prosp. Akad. Semenova 1, 142432 Chernogolovka, Moscow Region, Russian Federation.
E-mail: nav@icp.ac.ru (L M Nikolenko),
tel. (7-496) 522 12 88, e-mail: razumov@icp.ac.ru (V F Razumov)

Received 7 June 2012
Uspekhi Khimii **82** (5) 429 – 448 (2013); translated by A M Raevskiy

† A solar cell is a device for solar energy conversion to electricity using photoelectric effect, a one-piece module made of cells.

including printing techniques and high-performance roll-to-roll method.

The variety of designs of quantum dot solar cells includes the following main types:

— Schottky solar cells based on metal/semiconductor junctions;

— bulk QDs/conjugated polymer heterojunction solar cells;

— semiconductor/semiconductor heterojunction solar cells; and

— QD-sensitized solar cells.

Recently, there has been considerable progress in the field and numerous publications including analytical reviews are reported yearly. For instance, Talapin *et al.*[13] considered various QD-based optoelectronic devices including solar cells. A number of reviews are devoted to particular types of solar cells, such as hybrid QD/conjugated polymer solar cells,[14,15] QD-sensitized solar cells[16] and solar cells based on lead chalcogenides.[17,18] Various types of solar cells have been discussed in another study[19] whose authors focussed on QD-sensitized systems.

The highest solar energy conversion efficiency values for the solar cell types listed above are given in Tables 1 and 2. Of course, the η values attained by QD-based devices are still lower than those of Si-based converters (see above); however, one can hope that the former will substantially increase in the nearest future.

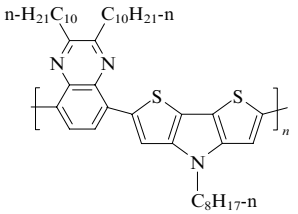
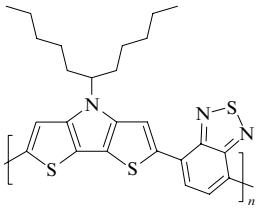
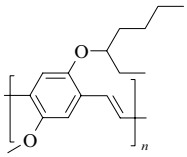
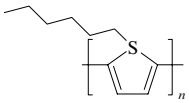
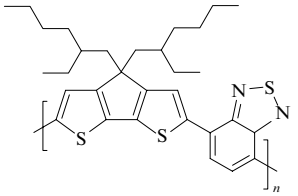
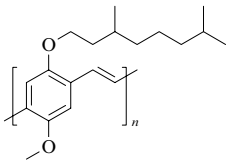
In this review, we report the results and recent advances in the design of solar cells based on QDs. We systematize modern solar cell architectures, classify them into main types and consider the principles of operation and parameters for each type of solar cells. We will discuss main problems and promising avenues of research aimed at improving solar cell parameters. The emphasis will be placed on surface modification of QDs and on the effect of the surface ligands on the properties of solar cells. Also, we will consider problems related to fabrication of QDs, charge transport properties of layers of quantum dots, as well as the role of 'hot' charge carriers in them.

Table 1. Energy conversion efficiency values for the best solar cells based on QDs.

Solar cell	η (%)	Ref.
Schottky cells		
ITO/PbS QDs/LiF/Al/Ag	3.6	20
ITO/PbSe QDs/Mg/Ag	3.6	21
ITO/PbS QDs/LiF/Al	3.8	22
ITO/$PbS_{0.7}Se_{0.3}$ QDs/Al	3.3	23
ITO/CdTe nanorods/Al	5	24
Bulk QDs/conjugated polymer heterojunction cells		
ITO/PEDOT : PSS/CdSe QDs – PCPDTBT/Al	2.7	25
ITO/PEDOT : PSS/PbS QDs – PDTPBT/Al	3.78	26
ITO/PEDOT : PSS/PbS QDs – PDTPQx/Al	0.55	27
ITO/PEDOT : PSS/CdSe nanorods – P3HT/Al	2.65	28
ITO/PEDOT : PSS/CdSe tetrapods – PCPDTBT/LiF – Al	3.13	29
ITO/PEDOT : PSS/hyperbranched CdSe QDs –P3HT/Al	2.2	30
ITO/PEDOT : PSS/CdSe tetrapods – OC_1C_{10}-PPV/LiF – Al	2.8	31
ITO/PEDOT : PSS/CdS QDs – P3HT nanowires/hole-blocking layer/Mg – Ag	4.1	32
Semiconductor/semiconductor heterojunction cells		
FTO/TiO_2/PbS QDs/Au	5.1	33
ITO/ZnO nanocrystals/PbS nanocrystals/Au	2.94	34
ITO/PEDOT : PSS/PbSe nanocrystals/ZnO nanocrystals/Al	3.4	35
FTO/TiO_2/PbS QDs/Au	5.5	36
ITO/CdTe nanorods/CdSe nanorods/Ca – Al	2.9	37
FTO/Zr-doped TiO_2/PbS QDs/Au/Ag	5.69	38
FTO/TiO_2 nanocolumns/PbS QDs/Au/Ag	5.6	39
FTO/Zr-doped TiO_2/PbS QDs shelled with Br ions/Au	6	40
QD-sensitized solar cells		
FTO/TiO_2/Sb_2S_3/P3HT/Au	5.13	41
FTO/TiO_2/CdS@CdSe/polysulfide electrolyte/Cu_2S	4.92	42
FTO/TiO_2/CdTe@CdS/polysulfide electrolyte/Au	3.8	43
ITO – poly(ethylene terephthalate) (flexible electrode)/TiO_2/CdS – CdSe QDs/polysulfide electrolyte/Cu_2S	3.47	44
TiO_2/CdSe ruthenium sensitizer/cobalt electrolyte/Pt	4.76	45
FTO/TiO_2/CdSe/polysulfide electrolyte/carbon nanospheres	3.9	46
FTO/TiO_2/Mn-doped CdS – CdSe/polysulfide electrolyte/Cu_2S/reduced graphene oxide	5.42	47

Note. Notatons are as follows: ITO is tin-doped indium oxide; FTO is fluorine-doped indium oxide; PEDOT : PSS is poly(3,4-ethylenedioxythiophene) doped with poly(styrene sulfonate); for other notations, see Table 2.

Table 2. Some properties of conjugated polymers used in solar cells.

Name	Molecular formula	LUMO [a] /eV	HOMO [b] /eV
Poly(2,3-didecylquinoxaline-5,8-diyl-*alt*-*N*-octyldieno-[3,2-*b*:2′,3′-*d*]pyrrole (PDTPQx)		−2.61	−4.64
Poly{2,6-[*N*-(1-octylnonyl)dithieno-[3,2-*b*:2′,3′-*d*]pyrrol]-*alt*-4,7-(2,1,3-benzothiadiazole)} (PDTPBT)		−3.08	−4.89
Poly[2-methoxy-5-(2-ethylhexyl)oxy-*p*-phenylenevinylene] (MEH-PPV)		−2.9	−5.3
Poly(3-hexylthiophene) (P3HT)		−3	−4.9
Poly{2,6-[4,4-bis(2-ethylhexyl)-4*H*-cyclopenta[2,1-*b*;3,4-*b*′]dithiophene]-*alt*-4,7-(1,2,3-benzothiadiazole)} (PCPDTBT)		−3.5	−4.9
Poly[5-(3,7-dimethyloctyloxy)-2-methoxy-*p*-phenylenevinylene] (OC_1C_{10}-PPV)		−2.8	−5.0

[a] Lowest unoccupied molecular orbital. [b] Highest occupied molecular orbital.

II. Parameters determining the efficiency of solar energy conversion

The operation of a solar cell is based on charge separation at the interface between the electron-donating and electron-acceptng materials. Conversion of solar energy to electricity involves the following main steps determining the efficiency of a photovoltaic device:

— light absorption by the active layer;

— formation of electron – hole pairs (excitons) and their subsequent diffusion towards the donor/acceptor interface;

— dissociation of an exciton to a hole and an electron;

— transport of charge carriers throughout corresponding phases towards electrodes.

Typical light and dark $I-V$ curves of a photovoltaic device are shown in Fig. 1.

Absorption of a photon is followed by creation of an exciton, which dissociates to an electron and a hole at the interface. Accumulation of charge in the space between electrodes creates a potential difference. As a load is connected, an electric current flows in the external circuit. As the load resistance increases, the solar cell potential changes from zero (at short circuit, one has $R \to 0$) to the open-chain potential V_{oc}. At the same time, the electric current changes from its maximum value (short-circuit current I_{sc}) to zero. The main parameters of the $I-V$ curve, which are used to characterize the operation of solar cells, include the short-circuit current, the open-circuit voltage and the fill factor (FF).

The short-circuit current is given by the product of the density of charge carriers (n) produced upon exposure to light by the mobility of charge carriers (μ) and by the electric field (E) acting on charge carriers

$$I_{sc} = e n \mu E$$

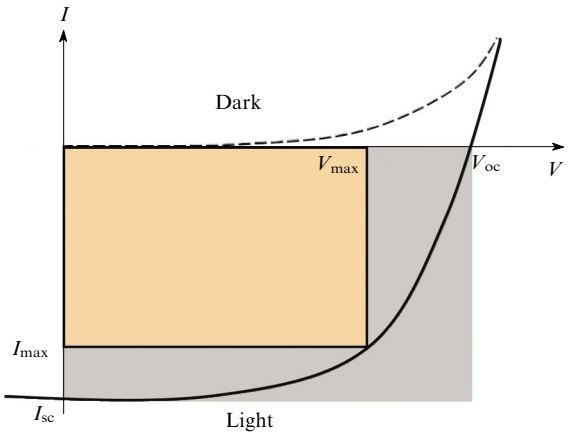


Figure 1. Current–voltage curve of a solar cell.

The I_{sc} parameter characterizes the maximum number of photogenerated charge carriers which produce electric current in the external electric circuit and, hence, depends on the absorption spectrum of the photoactive substance. Usually, the short-circuit current density (J_{sc}/A cm^{-2}) is specified; this allows different solar cells to be compared.

The open-circuit voltage depends on various factors which will be discussed below for each particular type of solar cells. They first of all include the electronic properties of materials and electrodes used.

The maximum power produced by a solar cell is given by

$$P_{max} = I_{max}\, V_{max}$$

and it corresponds to a particular point on the $I-V$ curve.

The fill factor characterizes the degree of perfection of the $I-V$ curve and is given by

$$FF = \frac{I_{max} V_{max}}{I_{sc} V_{oc}}$$

The efficiency of solar energy conversion is the key parameter characterizing a solar cell (and, therefore, its operation). It is defined as the ratio of the maximum power to the power of incident light (P_{in})

$$\eta = \frac{P_{max}}{P_{in}} = FF\,\frac{I_{sc} V_{oc}}{P_{in}}$$

Yet another important parameter is the external quantum efficiency (EQE)‡ equal to the ratio of the number of electrons arriving at electrodes to the number of incident photons. The EQE is 100% if each incident photon creates an electron–hole pair which then dissociates. However, the EQE of actual devices is much lower than 100% owing to losses due to reflection of incident photons and to recombination of charge carriers. But the EQE value can also be higher than 100% for, *e.g.*, those devices in which an absorbed photon creates more than one electron–hole pair, in particular, due to multiplication of charge carriers (see below).

‡ It is also called Incident Photon to Current Efficiency (IPCE).

To compare different types of solar cells, tests are performed under standard conditions, *viz.*, at a cell temperature of 25 °C under irradiation with light with the model solar radiation spectrum AM1.5 and a radiation power of 100 mW cm^{-2}. The standard model solar radiation spectrum AM1.5 corresponds to an average power and spectal characterstics of solar light at the Earth's surface at a solar zenith angle of 48.2°.

To improve the light conversion efficiency, there has been a research on various novel electron-donating and electron-acceptng materials and their combinations. There is considerable recent literature on utilization of QDs as promising photoactive components; unique electronic and optical properties of QDs offer new prospects for physicochemical design of solar cells. In particular, owing to the quantum size effect one can vary the bandgap width (E_g) by varying the QD size; this will allow one to optimize absorption of solar radiation. By varying the QD size one can also control positions of the energy levels of QDs relative to the energy levels of other solar cell components and thus control charge transfer across the interface.

III. Synthesis of colloidal quantum dots

Semiconductor nanoparticles of specified size are synthesized by various methods involving nucleation and growth in supersaturated solutions.[48] Quantum dots utilized in solar cells are usually prepared by reactions of organometallic precursors at high temperature. This method was for the first time used by Murray *et al.*[49] to synthesize CdX (X = S, Se, Te) quantum dots; in particular, a cold (room-temperature) solution of selenium in trioctylphosphine (TOP-Se) was injected into a hot (300 °C) solution of dimethylcadmium ($CdMe_2$) in trioctylphosphine oxide (TOPO). Rapid addition of the cold TOP-Se solution led to avalanche-type formation of CdSe nuclei; the temperature of the mixture abruptly decreased to ~230–260 °C, and the nucleation ceased, followed by growth of all nuclei present in the system. High synthesis temperature (230–260 °C) favours thermal annealing of nanocrystals and formation of almost perfect crystal lattice.[50] This method satisfies two conditions necessary for the synthesis of high-quality QDs, *viz.*, separation in time of nucleation and nanoparticle growth and their thermal annealing; this makes it possible to obtain defect-free QDs with narrow particle size distribution and high quantum yield of fluorescence.

Unlike other liquid-phase methods, the high-temperature method allows one not only to obtain nanoparticles with rather narrow particle size distribution, but also to additionally narrow this distribution by controlling the particle growth during the synthesis. Under particular conditions, the nanocrystal size distribution during the growth can be narrowed (focusing mode) or broadened (defocusing mode).[51] To keep the focussing mode persistent, it was proposed to add reactants gradually, thus retaining the necessary degree of supersaturation in the solution throughout the synthetic procedure. The particle size distribution can also be focussed in another manner, *viz.*, by controlling the temperature of the synthesis. As temperature decreases, the solubility of most substances also decreases; therefore, the degree of supersaturation increases and the size of the critical nucleus decreases.[52] This method of controlling the growth of nanocrystals makes it possible

not to add additional reactants and to obtain monodisperse crystals 1.5–5 nm in size.

In the high-temperature colloidal method using organometallic precursors, nucleation and growth occur in solution in the presence of ligands that are adsorbed on the surface of growing crystals. Such ligands include not only alkylphosphines and alkylphosphine oxides (TOP, TOPO, tributylphosphine oxide), but also alkylamines (hexadecylamine, oleylamine), carboxylic (oleic, stearic) acids and phosphonic (tetradecylphosphonic, octadecylphosphonic) acids. Having appropriately chosen the experimental conditions (*i.e.*, a combination of the precursor, surfactant, solvent, temperature, *etc.*), one can use this technique to synthesize QDs of different composition including various nanocrystals, *e.g.*, $A^{II}B^{VI}$ [CdX, ZnX (X = S, Se, Te),[53–55] HgTe (Ref. 56)]; $A^{IV}B^{VI}$ [PbX,[57–61] SnX (X = S, Se, Te)];[62,63] $A^{III}B^{V}$ [InP,[64] InAs,[65] GaP (Ref. 66)], as well as $CuInS_2$ (Ref. 67) and $CuInSe_2$ (Ref. 68), *etc.* The method allows one to prepare nanoparticles of not only different composition and size, but also shape (*e.g.*, nanorods or nanotetrapods[69,70]).

It should be noted that solar cells can be fabricated from both pre-synthesized nanocrystals and grown in the polymer matrix[71,72] or those grown *in situ* on the surface of the photoanode.

IV. Charge transport properties of layers of quantum dots. Surface modification of quantum dots

As a rule, QDs in the active layer of solar cells are used as an individual phase or in the form of consolidated thin layers 100–300 nm thick, whose electron transfer properties play a decisive role in the attainment of high efficiency of solar energy conversion to electricity. Charge transport in such QD layers (phases) occurs by various mechanisms including electron tunnelling between adjacent QDs and variable range hopping where hopping distance takes random values. In more detail, charge transport in the systems in question was considered in another review.[73] Clearly, the interparticle distance plays a significant role for all mechanisms of transport in consolidated QD layers.

Quantum dots synthesized by the colloidal method are capped with a protective layer of surfactant molecules with long hydrocarbon chains to prevent coagulation of QDs. Therefore, an important step in the design of various photovoltaic devices consists in replacement of original surfactants by new surface ligands to shorten the distance between QDs and, therefore, to improve the charge transport properties. Usually, surface modification is performed using shorter organic molecules (pyridine, benzene-1,3-dithiol, benzene-1,4-dithiol, n-butylamine, tributylamine, octylamine, ethane-1,2-dithiol, mercaptopropionic and thioglycolic acids) containing functional groups that exhibit some affinity to the surface of QDs.

An increase in the mobility of charge carriers with a decrease in the interparticle distance was confirmed experimentally[74] for films of PbSe QDs capped with alkanedithiols having different-length hydrocarbon chains. Charge carrier mobility measurements of layers of QDs treated with different ligands gave the following ranges of mobility values: from 1×10^{-4} (Ref. 75) to 0.5–1.2 (Ref. 76) for electrons and from 1.5×10^{-3} (see Ref. 77) to 0.12–0.18 $cm^2\ V^{-1}\ s^{-1}$ (Ref. 78) for holes. The highest mobility values were obtained for hydrazine-treated layers of QDs. Also, processing of PbSe QDs capped with oleic acid in hydrazine led to an increase in the conductivity of QD layers by ten orders of magnitude.[78]

It should be noted that the conducting properties of layers of QDs depend on both the mobility and concentration of free charge carriers. Replacement of ligands on the surface of QDs can lead not only to shortening of the interparticle distance (and, therefore, to higher charge carrier mobilities), but also to doping of QD layers (*i.e.*, to an increase in the concentration of free charge carriers). The type and degree of doping are important parameters influencing the operation of photovoltaic devices. Doping of QD layers is related to formation of surface traps. Uncompensated surface ions (cations or anions) trapping free charge carriers act as donors if holes are trapped or as acceptors if electrons are trapped. The degree of doping is determined by the difference between the number of hole- and electron-trapping defects. Treatment of the surface of films with ligands as well as thermal annealing leads to changes in the number of all types of defects and, as a consequence, the overall type and degree of doping. For instance, hydrazine-treated PbSe QD films had n-type conductivity.[78] Vacuum treatment or thermal annealing led to changes in the conductivity type of the films. n-Butylamine PbS QDs exhibited p-type conductivity because oxides covering the surface of QDs acted as p-type dopants.[79] Subsequent treatment of these QDs with ethanedithiol cause the surface concentration of oxides to decrease, which led to a decrease in the concentrations of the main charge carriers.

The surface of QDs is modified with not only organic, but also inorganic ligands, *e.g.*, metal chalcogenide (SnS_4^{4-}, $Sn_2Se_6^{4-}$, $In_2Se_4^{2-}$, $Ge_4S_{10}^{4-}$) complexes. They can be used to significantly improve the electrical properties of layers of QDs compared to layers of QDs capped with organic ligands. A study of gold nanocrystals revealed a decrease in the interparticle distance from 2 to 0.5 nm and an increase in the conductivity by 11 orders of magnitude upon replacement of dodecanethiol by $Sn_2Se_6^{4-}$ as the surface ligand.[80] Halide ions were also used to passivate the surface of QDs.[40] The electron mobility in layers of QDs covered with a monolayer of halide ions was as high as $4\times10^{-2}\ cm^2\ V^{-1}\ s^{-1}$.

V. Multiple exciton generation and the role of 'hot' charge carriers in quantum dots

According to calculations by Shockley and Queisser,[2] the limiting efficiency of solar energy conversion to electricity in a single-junction solar cell is 30%. In this case, main losses are due to conversion of solar radiation to heat, incomplete absorption of radiation and recombination of charge carriers. The solar radiation spectrum corresponds to photons with energies in the range from 0.5 to 3.5 eV. Photons with energies lower than the semiconductor E_g value are not absorbed and not involved in the photocurrent. Photons whose energy is higher than E_g produce 'hot' charge carriers with an excess kinetic energy equal to the difference between the energy of photons and E_g. The excess energy transferred to electrons is converted to heat through electron–phonon coupling. The process leads to the greatest losses (47% for silicon with E_g = 1.1 eV), being the main factor limiting the efficiency of photovoltaic devices.

To reduce losses and approach an efficiency of about >31%, multi-junction (or 'tandem') solar cells were designed. They combine a number of p–n-junctions made of semiconductors with successively decreasing E_g values along the direction of light propagation. In such systems, photons with higher energies are absorbed by the semiconductors having higher E_g values, while low-energy photons are absorbed by semiconductors with lower E_g. The maximum conversion efficiency predicted for solar cells with an infinite number of junctions is 68% (*cf.* 43.5% as the best result obtained so far[81]). The efficiency of solar cells can be improved using 'hot' charge carriers in two ways:

— by increasing the open-circuit voltage; to this end, 'hot' charge carriers should be trapped by high-energy donors or acceptors of electrons or by electric contacts with corresponding work functions prior to converting the excess kinetic energy to heat by phonon radiation;

— through impact ionization (inverse Auger effect). In this case, a 'hot' charge carrier produces two or more electron-hole pairs; as a consequence, the short-circuit current can be considerably increased (Fig. 2).

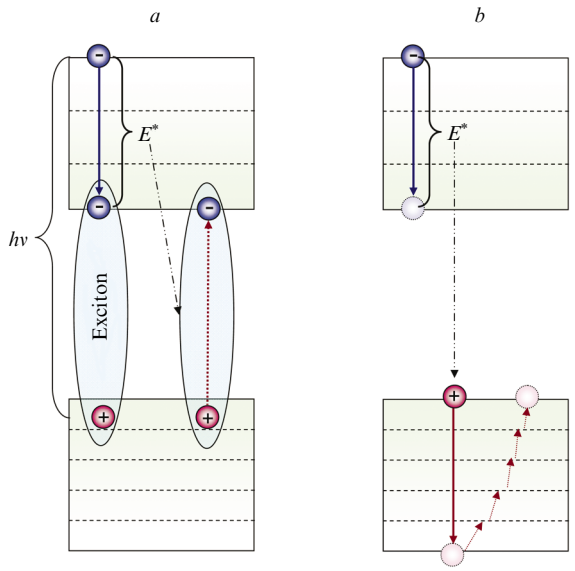


Figure 2. A schematic of multiple exciton generation (*a*) and Auger relaxation (*b*).
Excess kinetic energy (E^*) is consumed to generate additional excitons (*a*) or is transferred to a hole which then relaxes (*b*).

Realization of these mechanisms requires that the processes be faster than relaxation of 'hot' charge carriers through electron–phonon coupling. In bulk semiconductors, 'hot' charge carriers are thermalized rapidly, *e.g.*, the relaxation time for silicon is about 1 ps.[82] Uniqueness of QDs consists in that owing to the quantum size effect, the conduction band and the valence band represent discrete energy levels rather than continuous sets of energy states. The energy difference between these levels becomes much larger than the characteristic phonon energies. Thus, cooling of 'hot' charge carriers in QDs should occur at the expense of simultaneous radiation of a large number of phonons.

This process is little probable; therefore, it was assumed that cooling of 'hot' charge carriers in QDs is significantly slowed down. The effect was called 'phonon bottleneck'. However, a number of experiments revealed rather short relaxation times of charge carriers in QDs ranging from about 100 to 500 fs.[83–85] Also, it was found that as the size of QDs decreases, the relaxation rate increases rather than decreases although the energy difference between the levels increases. The effect observed is due to realization of alternative channel of cooling of 'hot' charge carriers through Auger relaxation accompanied by efficient electron–hole energy transfer owing to strong Coulomb interaction between them.[83,86] Relaxation of a hole in the valence band is fast due to the higher density of states (see Fig. 2 *b*). Faster relaxation in small QDs can also be explained by strengthening of electron–hole Coulomb interaction.

The electron–hole interaction force can be reduced by surface modification of QDs. For instance, replacement of TOPO by pyridine on the surface of QDs causes the relaxation time of 'hot' charge carriers to increase from 1 to 200 ps.[87]

In lead chalcogenide QDs, the exciton Bohr radius is large and, therefore, the motion of charge carriers is strongly confined in space, the energy levels of holes and electrons are distant from one another, and Auger relaxation is thus little probable. However, no 'phonon bottleneck' effect is observed; this can be explained by relaxation through surface states or by impact ionization. Impact ionization (multiple exciton generation) is a process where a high-energy exciton created in a semiconductor upon absorption of a photon with the energy $E > 2E_g$ produces two excitons with energies equal to E_g through transfer of the excess energy to an electron in the valence band. This type of energy transfer allows two or more excitons to be created upon absorption of a single photon. Multiple exciton generation was observed in PbSe,[88,89] PbS,[89] PbTe,[61] CdSe[90] and InAs[91] QDs. A study of lead selenide revealed generation of seven excitons upon absorption of a photon with $h\nu = 7.8\,E_g$ for $E_g = 0.636$ eV.[92]

Devices based on PbSe QDs with multiple exciton generation were reported.[93] The EQE values exceeded 100%, the highest being equal to 114%. However, the possibility of considerable increase in η due to multiple exciton generation casts some doubt. In particular, it was shown that utilization of PbSe QDs leads to only 2% increase in the efficiency due to multiple exciton generation.[94]

VI. Schottky-junction solar cells

One of the simplest types of photovoltaic devices based on QDs utilizes the Schottky junction, *i.e.*, a contact between two materials, a p-type semiconductor and a metal with low work function (Al, Ca, Mg) or an n-type semiconductor and a metal with high work function (Au, Pt). Usually, such a device is a layer of QDs (active layer) placed between two electrodes. The active layer is needed for light absorption and generation of electron–hole pairs. The authors of most studies on the topic employed QDs with p-type conductivity and metals (Al, Ag) as electrode material.

The design of a device and the energy diagram of a Schottky solar cell is shown in Fig. 3. Since the Fermi levels

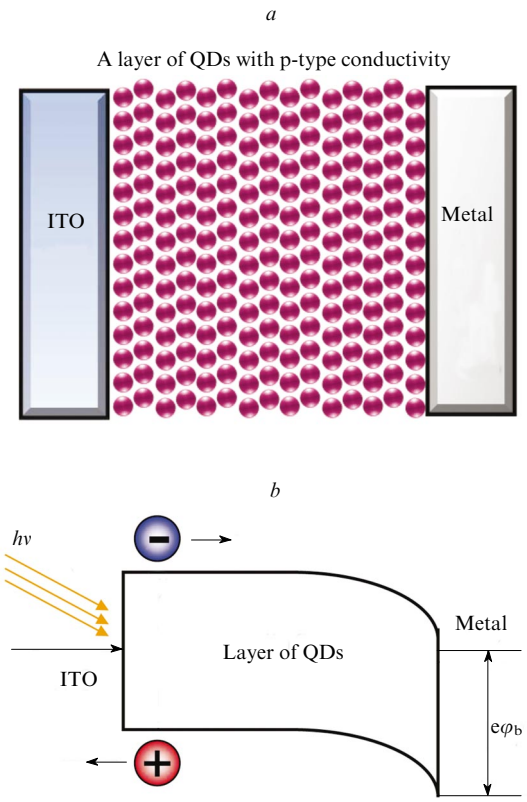


Figure 3. A Schottky solar cell (*a*) and its energy diagram (*b*). φ_b is the Schottky barrier height.

of the p-semiconductor and the metal with low work function have different positions, their contact causes electrons to flow from the metal to the semiconductor. A region depleted of the main charge carriers appears in the near-boundary layer of the semiconductor; the concentration of the main charge carriers will uniformly increase on going from the surface into the interior of the semiconductor. This situation corresponds to downward-bent bands in the energy diagram which characterizes the change in the potential in the depletion layer and equal to the work function difference between the metal and semiconductor. When exposed to light, the Schottky junction favours dissociation of excitons formed and escape of electrons from the active layer. Anodes represent optically transparent conducting materials with high work function (usually, these are tin- or fluorine-doped indium oxide, ITO or FTO, respectively), which form Ohmic contacts with semiconductors and favour extraction of holes.

A detailed study [77] on the operating mechanism of such solar cells revealed that an important role in the device is played by charge carrier drift in the depletion layer driven by the contact potential difference and by diffusion of charge carriers in the quasi-neutral layer. The operating efficiency of such a device depends on the balance between the light absorption and charge extraction. Generation and separation of most charge carriers occur in the depletion layer 150 nm wide. Under the action of the contact electric field, electrons flow to the metallic electrode while holes move to the edge of the depletion layer and diffuse towards the ITO surface. Transport in the depletion layer can be considered efficient because the drift length is 10 μm for holes and 1 μm for electrons. As the thickness of the active layer increases, light absorption also increases, but transport in the thicker layer is influenced by the diffusion rate of charge carriers in the neutral region. This effect becomes pronounced if the active layer thickness for the device approaches the sum of the minor charge carrier diffusion length and the width of the depletion layer. The electron diffusion length in the neutral region is 0.1 μm, so the efficiency decreases at thicknesses >300 nm.

Currently, Schottky solar cells are mainly fabricated from nanomaterials absorbing in the IR spectral region, *e.g.*, PbS, PbSe, CdTe. Research groups headed by Nozik and Sargent contributed largely to fabrication of this type of devices. Sargent and co-workers [95] reported one of the first studies on Schottky solar cells [$\eta = 1.8\%$ (AM1.5G)]. The active layer included 6-nm PbS nanoparticles prepared by the colloidal method using organometallic precursors. The starting oleic ligand was replaced by the shorter-chain n-butylamine. Quantum-dot films 230 nm thick were applied to ITO-covered glass substrate by the spin-coating method in inert atmosphere. The Schottky junction was formed between the QD film and the aluminium layer 140 nm thick deposited by thermal evaporation. Prior to aluminium deposition, the surface of the QDs film was covered with a thin (0.7 nm) LiF layer to improve the operating properties of the device .

A PbSe QD film on a glass substrate covered with ITO by the layer-by-layer deposition was used;[96] calcium, magnesium, silver, aluminium and gold were used as electrodes. The ITO-covered substrate was first immersed in a solution of QDs in hexane and then in a solution of ethane-1,2-dithiol (EDT) in acetonitrile to remove oleic ligands. The use of methylamine instead of EDT gave similar results. The best device operating in nitrogen atmosphere was characterized by $J_{sc} = 24.5$ mA cm^{-2}, $V_{oc} = 0.239$ V, FF $= 0.41$ and $\eta = 2.1\%$.

It was also confirmed [96] that performance of this solar cell configuration is based on Schottky junction. In this case, the open-circuit voltage should be a linear function of the height of the energy barrier ($e\varphi_b$), and for the contact between the p-type semiconductor and a metal one has

$$e\varphi_b = E_g + e(\chi - \varphi_M)$$

where e is the electron charge, χ is the electron affinity of the semiconductor and φ_M is the work function of the metal.

For various cells based on different-size QDs, it was shown that V_{oc} (in Volts) linearly increases with increasing the QD bandgap

$$V_{oc} = 0.49\frac{E_g}{e} - 0.253$$

A decrease in V_{oc} with increasing the work function of the metallic contact served yet another proof of validity of the model based on Schottky junction for this configuration. However, going from gold to calcium ($|\Delta\varphi_M| = 2.3$ eV) caused the open-circuit voltage to increase by only 0.15 V. This can be explained by Fermi level pinning; as a result, the height of the energy barrier is almost independent of the work function of the metal. Often, the Schottky barrier is formed by defects that appeared at the interface during deposition of the metal. Probably, this is just the case. To date, the maximum

efficiency attained for this type of photovoltaic devices is ~3%–4%.

An important problem in the design of Schottky solar cells is to make the system more stable to oxygen. The first solar cells with junctions based on n-butylamine-capped PbS QDs degraded in air during a few minutes.[95] A possible reason for low stability of the devices consists in insufficient passivation of the surface of QDs. Labile ligands, such as n-butylamine and ethanedithiol, inefficiently protect QDs from oxygen and moisture. Oxidation of the surface of QDs leads to the appearance of deep electron traps acting as recombination centres; they can hamper electron transfer. This problem can be solved using a bidentate ligand *N*-(2,4,6-trimethylphenyl)-*N*′-methyldithiocarbamate containing a dithiocarbamate group which forms a strong bond with the metal cation on the surface of QDs and readily replaces oleic acid. A η value of 3.6% was thus obtained.[20] Passivation of the surface of QDs with thiophenol that strongly interacts with the surface of QDs made it possible to fabricate cells with $\eta = 3.6\%$ and to increase their operating life to a few weeks in inert atmosphere and to a few hours in air.[21]

A comparable efficiency of solar energy conversion using cells operating in nitrogen atmosphere was attained by improving the methods of synthesis of PbS QDs.[22] It was shown that the growth rate of QDs governs the quality of synthesized particles and, therefore, significantly influences the η value. The growth rate was controlled by varying the concentration ratio of the lead and oleic acid (the acid was used as stabilizing ligand). At low growth rate, monodisperse stable nanocrystals with low concentration of traps were obtained. The efficiency of cells based on QDs synthesized under these conditions reached a value of 3.8%, being twice as high as the efficiency of cells based on QDs synthesized at high growth rate.

The operating stability of solar cells is, in particular, affected by the state of the interface between the active layer and metallic electrode. Metals characterized by low work function are readily oxidized and can interact with ligands on the surface of QDs. For instance, aluminium (4.2 eV) or silver (4.3 eV) was used as cathode in solar cells based on PbS QDs.[97] Utilizing less reactive silver improved the solar cell stability compared to that of cells with Al cathodes. However, solar cells with the silver electrode (the work function of Ag is higher than that of Al) were characterized by lower V_{oc}. It was proposed to use a thin buffer layer between the active layer and the Al electrode. Among the buffer layers studied (SiO, $BiCl_3$, LiF), the best effect was obtained with LiF. A LiF thin layer (thickness 0.8 nm) made it possible to slow down oxygen diffusion and the oxidation of the CD/metallic electrode interface. Solar cells thus produced were characterized by $\eta = 2\%$ and a tenfold longer operating life (to tens of hours) in air.

An efficiency of 3.6% was also obtained using a magnesium electrode with a low work function (3.6 eV).[21] Experiments with a gold electrode (5 eV) revealed no formation of the Schottky junction and the $I-V$ dependence was linear.

Kuo *et al.*[98] proposed yet another approach to increasing the operating life and efficiency. The use of additional hole transfer layer based on PEDOT : PSS in a cell with the PbSe QDs active layer and Al/Ca cathode made it possible to increase the η value from 1.5% to 2.4%; the operating life showed a sixfold increase to 2 h. The increase in V_{oc} is explained by a specific mutual position of the energy levels of QDs, PEDOT : PSS and ITO, which favours hole transport to the anode. The increase in I_{sc} is due to the more smooth anode surface (improved contact between the electrode and the active layer as well as charge transport).

The active layer of a Schottky solar cell can comprise nanocrystals of not only binary compounds. For instance, solar cells based on PbS_xSe_{1-x} nanocrystals appeared to be more efficient than those based on undoped PbS and PbSe, *viz.*, higher I_{sc} and V_{oc} values were obtained.[23] The best devices based on $PbS_{0.7}Se_{0.3}$ nanocrystals were characterized by $\eta = 3.3\%$ at $J_{sc} = 14.8$ mA cm^{-2}, $V_{oc} = 0.45$ V and FF = 0.5.

Most Schottky solar cells are fabricated using lead chalcogenides; however, it was also shown that cells based on CdSe are more stable than those based on PbSe.[96] The highest efficiency $\eta = 5\%$ was obtained using CdTe nanorods.[24] It was also pointed that charge transport and optical absorption were improved by annealing nanoparticle films, which led to their aggregation, changes in the properties of the material and to disappearance of the quantum size effect.

The conversion efficiency attained using Si nanocrystals instead of metal chalcogenide nanocrystals[99] was low, *viz.*, $\eta = 0.02\%$ at $J_{sc} = 0.148$ mA cm^{-2}, $V_{oc} = 0.51$ V and FF = 0.26.

VII. Hybrid quantum dots/conjugated polymer heterojunction solar cells

1. The architecture and principle of operation

The architecture of hybrid solar cells is similar to that of organic polymer–fullerene cells; they represent an active layer comprising a mixture of a conjugated polymer and nanocrystals placed between two electrodes (Fig. 4). The energy diagram of such a cell is shown in Fig. 5. Light absorption leads to generation of excitons in both the semiconductor and polymer, thus making this type of solar cells different from traditionally used polymer–fullerene cells in which fullerene does not contribute largely to absorption. The efficiency of charge separation and the η value depend strongly on the mutual position of the energy levels of the components of the active layer and electrodes. Dissociation of excitons at the nanocrystal/polymer inter-

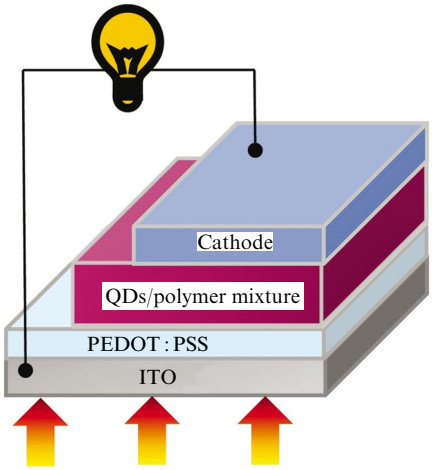


Figure 4. Device solar cell based on QDs/conjugated polymer heterojunction.

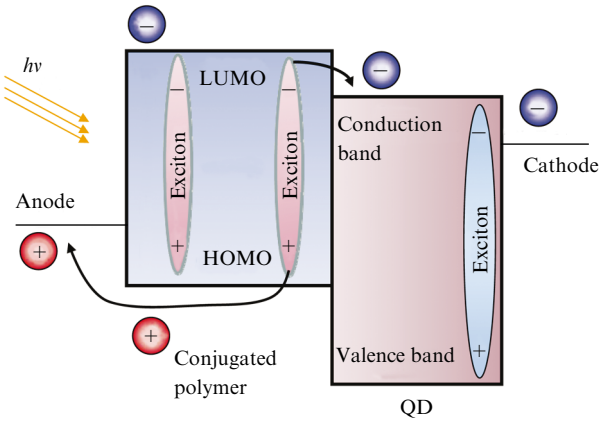


Figure 5. Energy diagram of a solar cell based on QDs/conjugated polymer heterojunction.

face is energetically favourable if the bottom of the conduction band of the nanocrystal is lower than the lowest unoccupied molecular orbital of the polymer while the highest occupied molecular orbital of the polymer is above the top of the valence band of the nanocrystal. Efficient dissociation requires that the energy difference between these levels be larger than the exciton binding energy. As a result of exciton dissociation, electrons from the polymer are injected into the semiconductor nanoparticle phase while holes from the semiconductor move to the polymer. The maximum possible open-circuit voltage of such a solar cell is proportional to the energy difference between the bottom of the QD conduction band and the polymer HOMO.

Usually, this type of solar cells utilizes Al, LiF/Al, Ca/Al or Mg as cathode, the metal chosen should form an Ohmic contact with the semiconductor. Optically transparent anodes are covered with a buffer material, namely, a PEDOT : PSS conducting polymer, to smooth the ITO surface and to improve adhesion of the active layer.

The exciton diffusion length in the polymer is ~10–20 nm on the average. Efficient charge separation requires that excitons be generated near the QDs/polymer interface, at a distance no longer than the characteristic exciton diffusion length. Also, light absorption is efficient if the polymer layer is at least 100 nm thick. This problem can be solved using the concept of bulk heterojunction (Fig. 6), which was for the first time proposed for polymer–fullerene solar cells.[100] A bulk heterojunction is formed by continuous interpenetrating n- and p-semiconductor phases. This causes the surface area of the interface to increase considerably; therefore, the distance from the exciton to the interface decreases. In this case, the thickness of the active layer can be rather large to ensure efficient absorption of solar radiation and charge separation in the whole volume of the active layer. Micrographs of the cross-sections of films with bulk heterojunctions formed by conjugated polymer P3HT with spherical and rod-like CdSe QDs are shown in Fig. 7.

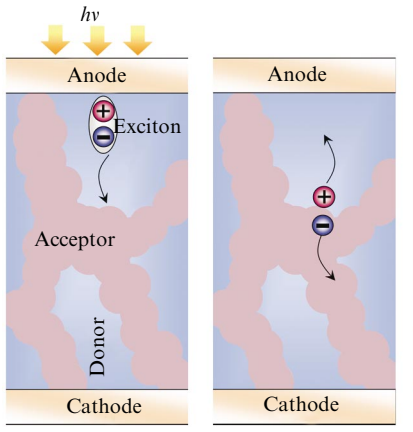


Figure 6. Illustration of processes in a bulk heterojunction solar cell.[100]

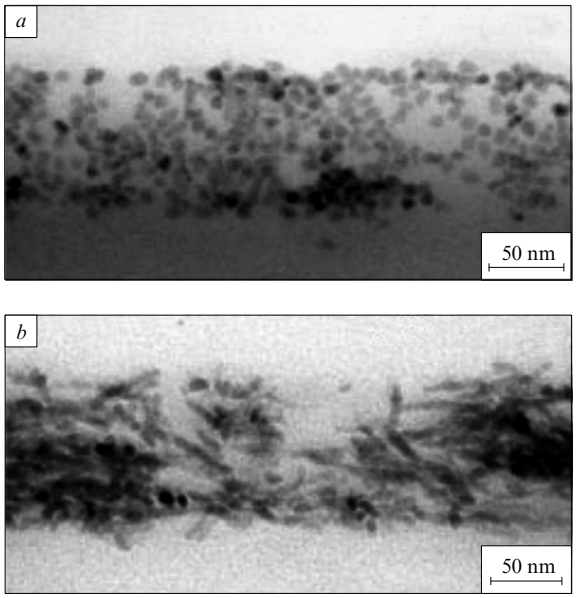


Figure 7. Micrographs of cross sections of polymeric composites containing spherical (*a*) and rod-like CdSe QDs (*b*).[101]

To date, most available studies on the design of solar cells based on QDs are devoted to just the hybrid cells based on polymer/QD heterojunctions. Investigations are mainly focussed on the search for new combinations of polymers and QDs, modification of the surface of QDs and on control of the morphology of the active layer.

2. Polymers and quantum dots used in hybrid solar cells

The properties of the conjugated polymer significantly affect the solar cell efficiency. The most important parameters are the E_g value of the polymer and position of the HOMO. Utilization of narrow-band conjugated polymers extends the spectral range of absorption and, therefore, the photocurrent increases. The open-circuit voltage depends on the energy difference between the bottom of the conduction band of QDs and the polymer HOMO. Therefore, the latter should be as low relative to the electron energy in vacuum (E_{vac}) as possible. The structural formulas of the polymers mentioned in this review and the corresponding HOMO and LUMO positions are presented in Table 2.[102–106]

Solar cells based on QDs and a conjugated polymer were for the first time fabricated in 1996.[107] The active layer comprised a mixture of 5-nm CdSe QDs and the polymer MEH-PPV. The solar energy conversion efficiency was as low as 0.1%. At present, the maximum η value for this type of solar cells with spherical CdSe QDs and the narrow-band polymer PCPDTBT is 2.7% at $V_{oc} = 0.591$ V, $J_{sc} = 8.3$ mA cm^{-2} and FF = 0.56.[25] The properties of two systems containing different polymers, PCPDTBT and P3HT, were also compared.[25] It was shown that in the former case the energy conversion efficiency increases owing to improved correspondence between the absorption spectrum of the active layer and the solar radiation spectrum, which leads to higher short-circuit currents.

Hybrid solar cells most often use CdSe QDs because methods of their synthesis are well developed, these particles exhibit appropriate spectral properties and can act as good electron acceptors when combined with traditionally used conjugated polymers. However, recently researchers have focussed on narrow-band lead chalcogenides. It is believed that the use of these compounds will extend the operating range of solar cells to the IR region. Initially, solar cells based on QDs that absorb in the near-IR range and traditionally used polymers had very low η values of 0.04% (Ref. 108) and 0.001% (Ref. 109) for the devices with the active layer based on the P3HT/PbSe and P3HT/PbS QDs, respectively. Combining PDTPQx and PbS QDs gave an efficiency of 0.55% at $J_{sc} = 4.2$ mA cm^{-2}, $V_{oc} = 0.38$ V and FF = 0.34 (Ref. 27). The maximum efficiency attained for hybrid cells based on lead chalcogenides is 3.78%.[26] In these cells, the active layer is composed of a mixture of PbS QDs and a conjugated polymer PDTPBT; in addition, the metallic electrode and the active layer were separated by a hole-blocking TiO_2 layer.

Hybrid bulk heterojunction cells also use CdS,[71] TiO_2,[110,111] SnSe,[112] $CuInS_2$,[72] GaAs,[113] ZnS,[114] SnS_2,[115] ZnO,[116] Si nanocrystals[117] as electron-conducting component.

3. Control of the composite morphology

An important factor determining the efficiency of solar cells is the morphology of QDs/conjugated polymer composites. The active layer of a solar cell should comprise continuous interpenetrating phases, the polymer and QDs, with the characteristic domain size no greater than the diffusion length of charge carriers in a given phase. The active layer is most often deposited from solution. The morphology of the active layer depends on the preparation condtions (including the choice of solvent and the use of various additives) and on the treatment technique (including thermal annealing or solvent annealing), as well as on the QD shape and size and on the concentration ratio of the polymer–QD mixture components.

a. The shape and size of quantum dots and the concentration ratio of mixture components

The morphology of the active layer can be controlled using anisotropic nanocrystals (nanorods, tetrapods, various branched structures to create channels for directed transport of charge carriers). For instance, CdSe tetrapods with legs 50 nm long and 5 nm thick as well as CdSe rods 5 nm thick and 65 nm long were used as components of the active layer.[118] Under identical conditions, solar cells with tetrapods were more efficient than those with rods owing to improved electron transport properties. The geometry of CdS nanorods in hybrid solar cells based on P3HT plays a significant role, *viz*., the efficiency η increased from 1.8% to 2.6% as the length-to-diameter ratio increased from 1 to 4.[71] Solar cells based on P3HT and CdSe and CdTe tetrapods, as well as CdTe/CdSe heterostructures were studied.[119]

Presently, the maximum η values for bulk heterojunctions based on anisotropic QDs are as follows: 2.65% for CdSe nanorods,[28] 3.13% for CdSe tetrapods[29] and 2.2% for hyperbranched CdSe nanocrystals.[30] Also, mixtures of spherical and anisotropic nanocrystals can be used. For instance, devices based on a conjugated polymer and a CdSe QDs/nanorods (2 : 1) mixture are characterized by higher efficiency than devices based on particles of the same type.[120]

Nanowires fabricated from narrow-band semiconductor GaAs and P3HT polymer were used as the active layer.[113] It was shown that light absorption by nanowires made almost no contribution to the photocurrent. The main role of nanowires was to create a bulk heterojunction with vertical morphology of the active layer; here nanowires are concentrated in the upper part near the metallic cathode while the polymer phase is concentrated near the anode.

To create percolation pathways for transport of photogenerated charges to electrodes, QDs, irrespective of their shape, should aggregate in the composite. To create the optimum morphology of the active layer, one should control the degree of aggregation of nanocrystals in the polymer, which depends on the concentration of QDs in the mixture with the polymer. The optimum concentration of nanocrystals in the composite is rather high and is about 90 mass % for spherical,[25,29,121] rod-like[122] and tetrapod CdSe QDs.[119] Lower concentrations lead to inefficient percolation and poor electron transport, whereas higher concentrations lead to inefficient light absorption and low mobility of holes. The optimum concentrations of the SnS_2 and ZnO QDs in composites are 50 mass % (Ref. 115) and 67 mass % (Ref. 116), respectively.

The morphology of a composite is influenced by not only the shape and concentration of QDs in the composite, but also by the QD size. In particular, the short-circuit current can be increased by increasing the size of CdSe nanoparticles.[123] There are various reasons for an increase in the electric current, and first of all, more efficient absorption of solar radiation. The larger the QDs (they have lower E_g) the larger the number of excitons produced and, therefore, the higher the short-circuit current. Another reason is related to the morophological effect, namely, the percolation pathway of charge transport is formed more easily in the case of large particles provided equal QD concentrations. Also, the effect of surface defects on charge transport for large QDs is less pronounced.

b. Thermal annealing of the active layer

Fabrication of the photoactive layer usually involves thermal annealing of the polymer/QDs composite. A study of polymer–fullerene solar cells based on P3HT showed that if the annealing temperature is equal or higher than the glass transition temperature of the polymer, the morphology of the composite changes due to crystallization of polymer chains. Prior to annealing, the polymer is in amorphous state and its crystallization is hampered by the presence of fullerenes distributed over the whole volume of the layer.

Thermal annealing leads to crystallization of polymer chains and to displacement of isolated fullerene molecules that can contact one another from the polymer phase.[124] Other consequences of thermal annealing affecting the operation of the device include removal of residual solvent, a decrease in the concentration of traps at interfaces, smoothing of the film surface and improvement of contact with electrodes. Also, taking a PbS QDs/MEH-PPV composite containing octylamine-capped PbS nanocrystals as an example, it was shown that annealing can lead to removal of labile ligands from the surface of QDs and, consequently, to improved contact between adjacent QDs as well as between QDs and the polymer.[125]

Composites can be heat treated both prior to and after spraying the metallic cathode. However, a study[25] of CdSe QDs/PCPDTBT solar cells revealed that if thermal annealing is performed prior to deposition of the aluminium cathode, the efficiency of operation was not improved; otherwise, it increased from 0.5%–0.6% to 2.3% after the first and to 2.7% after the second annealing step. It was assumed that such a behaviour can be due to diffusion of aluminium or to chemical reactions occurring in the course of annealing and improving the contact between the photoactive material and cathode.[25]

c. The effect of solvent and additives

If the active layer is deposited by the spin-coating method, the morphology of the film depends strongly on the choice of solvent. Usually, high-boiling solvents are preferred since in this case the time necessary to obtain a dry film increases. As a result, the polymer structure becomes more ordered. For instance, deposition from slowly evaporating trichlorobenzene leads to formation of P3HT films with high degree of crystallinity, composed of fibres to a few micrometres long; also, inter-chain $\pi-\pi$ interaction becomes stronger and charge transport significantly improves.[126] The use of trichlorobenzene instead of thiophene and chloroform to deposit the active layer comprising P3HT and CdSe nanorods improves the EQE and I_{sc} ($\eta = 2.6\%$).[127] Solar cells based on OC_1C_{10}-PPV and CdSe tetrapods deposited from trichlorobenzene were characterized by $\eta = 2.8\%$.[31] The authors of that study revealed vertical phase separation with the formation of a layer with high concentration of tetrapods near the metallic electrode and a polymer-enriched layer near ITO.

d. Solvent annealing

The film drying time can be increased by treatment of the active layer with solvent vapours. To this end, after coating the substrate with the composite the film in the liquid phase is placed in a closed container with atmosphere saturated with solvent vapours. In this case, interpenetration of the donor and acceptor phase is improved, as under thermal annealing. This approach was used in fabrication of hybrid polymeric solar cells.[28] The efficiency of cells based on CdSe nanorods/P3HT treated with benzene-1,3-dithiol vapours increased by 70% compared to that of untreated cells. Improved operation was explained by replacement of ligands on the surface of QDs upon treatment with benzene-1,3-dithiol vapours.

4. Surface modification of quantum dots

Modification of the surface of QDs is an important step in the design of bulk heterojunction solar cells. Ligands used in the synthesis form an insulating layer on the surface of QDs. To ensure efficient transport of charge carriers and to improve the compatibility of QDs with the polymer matrix, the original ligands should be replaced by shorter-chain ones. Often amines (n-butylamine, tri-n-butylamine[128]) and nitrogen-containing aromatics, *e.g.*, pyridine are used as surface ligands for QDs.[28, 127] Pyridine is most widely used to modify the surface of metal chalcogenide QDs. Relpacement of ligands is usually incomplete, so a fraction of the original ligand is retained on the surface of QDs and the efficiency of solar cells depends on the number of ligand replacement cycles.[129] For instance, the amount of pyridine on the surface of CdSe QDs increases from 54% for a single ligand exchange reaction to 80% for three ligand exchange cycles. Despite the fact that the reaction leads to a greater extent of ligand exchange, which in turn improves charge transport, the efficiency η decreased. For instance, the second cycle of the ligand exchange reaction increases the degree of aggregation of QDs in the P3HT layer, which leads to more pronounced phase separation and the characteristic sizes of the phases become larger than the exciton diffusion length.[129] Reduced efficiency can also be due to an increase in the number of surface defects in particles with higher amount of pyridine on the surface.

Taking solar cells based on P3HT and TiO_2 nanorods as examples,[110] it was shown that the use of oligo(3-hexylthiophene)carboxylic acid as ligand allows the short-circuit current and efficiency to be doubled as compared to the devices utilizing pyridine.

Thiols represent another class of compounds frequently used as surface ligands. With thiols, one can significantly improve the parameters of inorganic solar cells;[21, 96] however, these compounds are rarely used in solar cells based on conjugated polymers and QDs. The operation of cells based on CdSe nanorods and P3HT polymer was improved by treating the active layer with benzene-1,3-dithiol vapours, which led to replacement of pyridine on the surface of QDs.[28] Also, the active layer was treated with a solution of ethanedithiol in acetonitrile to replace the original n-butylamine on the surface of CdS QDs.[32] The active layer was formed from a mixture of CdS QDs and presynthesized P3HT crystalline nanowires. This approach made it possible to improve the morphology of the composite and the electronic interaction between the polymer and QDs. The highest η for hybrid solar cells based on conjugated polymers and QDs is 4.1%.[32]

Surface ligands influence not only charge transport, but also the morphology of composites; therefore, the ligand used should ensure high compatibility of QDs with the polymer matrix. To improve compatibility, some authors propose to functionalize the polymer with groups that exhibit some affinity to the surface of QDs. For instance, replacement of pyridine by amino-functionalized P3HT improves the compatibility of the polymer and QDs.[130] Modification of P3HT with thiol groups also improves contact between QDs and the polymer.[131] Yet another method of improving compatibility is to use bifunctional ligands containing two groups, one having affinity to the surface of QDs and the other capable of interacting with the polymer.[132] In particular, a composite prepared involving molecular recognition between diaminopyrimidine-functionalized P3HT and thymine-capped CdSe QDs was reported.[133] In this composite, nanocrystals uniformly distributed in the polymer matrix formed an extended 3D

network, whereas mixtures with no specific interaction exhibited phase segregation on the submicrometre level. This strategy was used to prepare composites from aniline tetramer and CdSe nanocrystals functionalized with 4-formyldithiobenzoic acid,[134] P3HT with vinyl terminal groups and CdSe nanorods functionalized with aryl bromide ligands[135] or [(4-bromophenyl)methyl]dioctylphosphine oxide.[136]

In addition to traditionally used ligand exchange procedures, there are alternative methods of surface modification of QDs. A method for increasing the efficiency η of solar cells based on CdSe QDs/P3HT composite to 2% by treatment of hexadecylamine-capped QDs with hexanoic acid was proposed.[121] Also, the efficiency increased upon annealing of systems based on P3HT composite and CdSe QDs functionalized with *tert*-butyl-*N*-(2-mercaptoethyl)carbamate.[122] The higher efficiency is due to transformation of ligands on the surface of QDs to shorter-chain aminothiol in the course of annealing.

Cells with no ligand exchange are also available. For instance, hybrid polymeric solar cells with high energy conversion efficiency were fabricated.[137] In this case, the active layer comprised oleylamine-functionalized multiwalled carbon nanotubes covered with P3HT and PbS QDs. Nanotubes act as not only substrate for fixation of QDs, but also as electron acceptors; this improves electron transport to the electrode.

5. Buffer layers

Inorganic nanocrystals can be used not only as components of the active layer, but also as components of the transparent electrode. For instance, a solar cell based on a CdS nanocrystals/polymer P3HT composite[71] utilized the transparent electrode made of FTO covered with a layer of ZnO nanorods. The η value increased from 0.7% (no nanorods) to 1.8% upon coating with the ZnO layer and the short-circuit current density increased from 3.8 to 6.8 mA cm^{-2}. It was assumed that nanorods act as electron collectors (create directed charge transport) and reduce the average distance from the electron generation point to the transparent electrode. Using ZnO nanocrystals as cathodic buffer layer, the η value considerably increased (by 80% and 30% for solar cells based on 5-nm and 6.5-nm CdSe nanocrystals, respectively) and the operating life also increased.[138] Cells with no buffer layer degraded in air within a few hours, whereas those containing the ZnO layer showed only a 40% decrease in efficiency after 70 days. Degradation can be due to the following: the active layer and electrodes can react with oxygen and water, and absorption of UV photons in the presence of oxygen and water leads to photo-oxidation. The authors of that study believe that ZnO nanoparticles, first, slow down transport of oxygen and water to the active layer and, second, absorb UV radiation. They also state that the ZnO layer is more stable than the calcium or magnesium buffer layers.[138] The use of Cu_2O nanoparticles as anodic buffer layer between ITO and the ZnO nanocrystals/MEH-PPV active layer made it possible to increase the cell efficiency by 132% to $\eta = 2\%$.[139]

Hybrid devices based on nanocrystalline semiconductors and polymers utilize not only pre-synthesized QDs. In some cases, one can grow semiconductor nanorods on the electrode and then cover them with the polymer.[140] It should also be noted that there exist more complex architectures including various carbon nanostructures as additional components.[123, 137] Cells based on ternary mixture CdSe QDs/polymer/PCBM (PCBM is methyl [6,6]-phenyl-C_{61}-butanoate) are characterized by an energy conversion efficiency of 1.3%.[123] When this mixture is exposed to light, polymer and QDs can absorb photons and generate excitons; then, electron transfer from the polymer to CdSe or PCBM, and from CdSe to PCBM, or hole injection from CdSe into the polymer are possible. The content of QDs in this system is rather high, but the IPCE spectra exhibit no band characteristic of QDs. Therefore, it is believed that the increase in the cell efficiency is most probably due to the change in the morphology of the active layer.

VIII. Semiconductor/semiconductor heterojunction solar cells

Presently, semiconductor/semiconductor heterojunction solar cells (one or both semiconductors are in the nanocrystalline form) are thought to be among the most promising ones. Considerable attention is paid to cells with lead chalcogenide QDs/metal oxide heterojunctions because they are characterized by the highest efficiency among solar cells based on QDs.

In 2010, solar cells based on PbS and TiO_2 nanocrystals with the so-called depleted heterojunction and an efficiency of 5% were fabricated.[33] The design and energy diagram of such a cell are shown in Fig. 8. In this cell, the hetero-

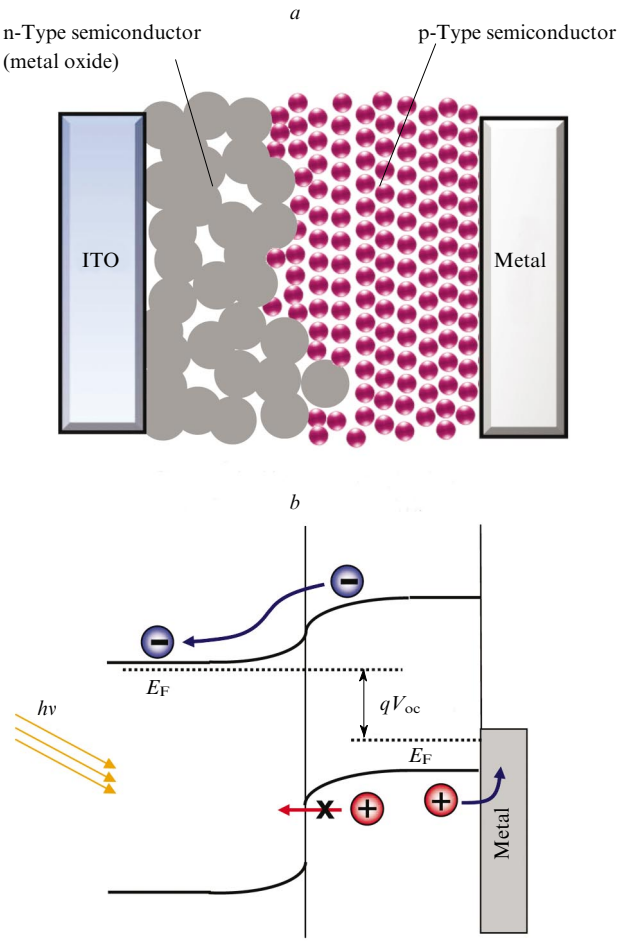


Figure 8. Depleted-heterojunction solar cell: a schematic (*a*) and energy diagram (*b*).[33]

junction is formed by the transparent layer of n-type semiconductor (TiO_2, ZnO) and the layer of QDs with p-type conductivity. Contact of these materials is accompanied by charge transfer from the oxide to the QDs layer, formation of a depletion layer and bending of energy bands. Excitons generated under exposure to light in the layer of QDs with p-type conductivity dissociate at the interface between two semiconductors. Injection of electrons into the metal oxide layer is due to the difference between the energy levels of the contacting layers and by the existence of the electric field produced by the p–n-junction. Free electrons are transferred across the metal oxide layer to the transparent electrode rather than the metallic electrode, as in the Schottky cells, while holes move to the contact between the layer QDs and the metal; this is the mechanism of creating inverse polarity. In these structures, the layer of QDs and the metallic electrode usually form an Ohmic contact; however, a Schottky junction can also be formed (as, *e.g.*, in a cell with the structure ITO/ZnO/PbS/metal) and affects the operation of the solar cell.[141]

Depleted heterojunction solar cells offer some advantages over Schottky cells. First, in the Schottky cells, the active heterojunction at which charge separation occurs, is near the metallic contact. In this case, excitons generated near the transparent electrode should travel across the whole QD film to arrive at the heterojunction; this leads to recombination losses. In the depleted heterojunction solar cells, the interface at which charge separation occurs is near the contact being irradiated, and the recombination losses are lower. Second, in this type of solar cells there is a barrier preventing undesired motion of holes from the layer of QDs to the metal oxide layer. Third, the open-circuit voltage in the Schottky cells is limited due to Fermi level resulting from the formation of defect states at the metal/semiconductor interface. In the depleted heterojunction, the TiO_2/QDs interface is passivated during the deposition of QDs.

Usually, fabrication of solar cells involves layer-by-layer deposition of QDs on a layer of TiO_2 nanocrystals. For instance, PbS QDs capped with oleic acid were deposited from an octane–decane mixture[33] and the each QD layer was treated with 3-mercaptopropionic acid in methanol. This led to replacement of oleic acid on the surface of QDs and they became insoluble in a specified mixture of solvents. This made it possible to perform eleven re-depositions and obtain a QD film 200 nm thick. The best device thus fabricated was characterized by $J_{sc} = 16.2$ mA cm^{-2}, $V_{oc} = 0.51$ V, FF = 0.58 and $\eta = 5.1\%$. It was shown that the open-circuit voltage is determined by the p–n-junction field potential (in this case, 0.52 V), which in turn depends on the energy difference between the Fermi levels of TiO_2 and PbS QDs.

The time of Förster-type energy transfer from one PbS QD to another was estimated as 200–400 ns.[33] Thus, Förster-type energy transfer cannot explain the efficient charge-carrier transport in films 200–250 nm thick because only a few QDs are involved in charge transport during the exciton lifetime (1–2 μs). It was concluded that charge transport in such layers is due to fast exciton dissociation in electric field produced by the p–n-junction and to hole and electron drift (or diffusion).

It was proposed to fabricate depleted heterojunction cells with a nickel electrode between TiO_2 and PbS QDs instead of gold electrode because the former is cheaper.[142] However, cells with the nickel electrode were of low efficiency due to the formation of metallic lead and NiS at the interface and to the formation of a Schottky junction precluding hole injection into nickel. The problem was solved using a LiF insulating intermediate layer. Cells with the LiF/Ni electrodes were as efficient as the reference cells with gold electrodes.

Depleted heterojunction solar cells were further improved by modifying the TiO_2 layer. A study[38] of the influence of doping TiO_2 with various metal ions (Mg, Sb, In, Al, Bi, Zr, Si, V, Pb, Nb) on the properties of TiO_2 revealed that doping with Sb and Zr significantly improves the efficiency of solar cells because position of the bottom of the conduction band of TiO_2 changes in such a manner that better conditions for electron injection from the layer of QDs into TiO_2 are created. The maximum efficiency of 5.69% was obtained for a cell based on PbS QDs/Zr-doped TiO_2 heterojunction.

Passivation of QD surface with inorganic ligands (halide anions) was proposed.[40] A procedure developed to obtain inorganic layers of QDs in which particles are covered with a monolayer of halide anions is carried out in air with no annealing. Such all-inorganic QD layers have energetically shallower trap states (surface states have lower energies relative to the energy of the bottom of the conduction band), the concentration of traps in them is lower while the charge-carrier mobility is higher than in the QD layers covered with organic ligands. This allowed record-high efficiency values to be obtained, *viz.*, 6% for cells with the FTO/Zr-doped TiO_2/Br^--shelled PbS QDs/Au structure and 4.5%, 5.54% and 2.95% for cells of identical structure and different anions (Cl^-, I^- and SCN^-, respectively).

Yet another promising method of making this type of cells more efficient is to form the active layer with a more complex geometry. In the solar cells considered above, the heterojunction is formed between planar semiconductor layers. Also, a bulk depleted heterojunction was reported.[36] In depleted heterojunction solar cells, efficient charge separation occurs at a distance equal to the width of the depletion layer from the interface. Therefore, a TiO_2/PbS bulk heterojunction cell was produced where the characteristic size of PbS domains did not exceed the width of the depletion layer (Fig. 9). For this architecture, the thickness of the active layer increases and extraction of corresponding charges into electrodes is not deteriorated; thickening of the active layer leads to an increase in absorption of solar radiation compared to absorption in the bilayer devices and the current density increases by 30% to 20.6 mA cm^{-2}. It was found that in such a device, efficient charge separation is attained if the difference between the energy levels of TiO_2 and PbS is larger than for planar devices. To decrease the energy of the bottom of the conduction band of TiO_2, the TiO_2 layer was treated with $TiCl_4$. Thus, practical implementation of the idea of bulk depleted heterojunction in semiconductor solar cells made it possible to fabricate solar cells with a very high efficiency of 5.5%.

A comparable efficiency ($\eta = 5.6\%$) was obtained using a structurally ordered TiO_2 electrode in the form of nanocolumns grown on a substrate coated with FTO.[39] Nanocolumns are organized in such a fashion that each column is equally spaced from its neighbours by a distance $d \approx 275$ nm. This distance meets the condition

$$d \approx 2W + L$$

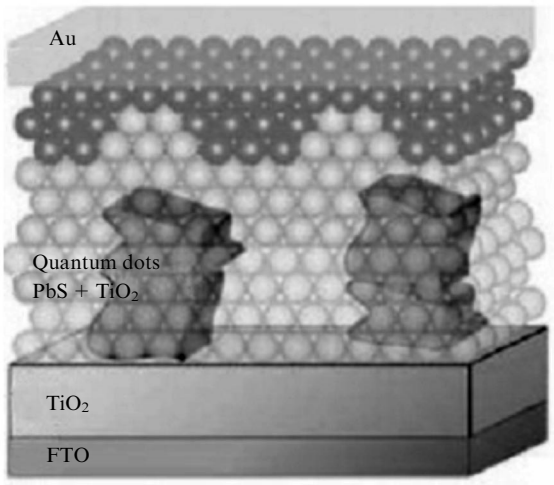


Figure 9. Depleted bulk heterojunction solar cell: a schematic.[36]

where W is the width of the depleted region in the layer of QDs and L is the diffusion length of minority charge carriers (electrons) in the QD film.

This architecture enables efficient collection of charges because all of them are photo-generated in the depletion layer or near it.

Thus, a bulk depleted heterojunction uses a larger amount of QDs in the layer for better light absorption, being also characterized by efficient charge separation (*i.e.* most excitons generated dissociate and charge carriers reach corresponding electrodes).

Zinc oxide is a good candidate for being a transparent n-type semiconductor.[24] To fabricate a solar cell, a layer of ZnO nanocrystals (100 nm thick) was deposited on a substrate covered with ITO by spin-coating. Quantum dots (PbS) were deposited by multiple immersion of the substrate into a solution of quantum dots in hexane and subsequent treatment with ethanedithiol. Solar cells thus obtained were characterized by $\eta = 2.94\%$, being highly stable in air, namely, the η value remained unchanged after 1000-h irradiation in air. Solar cells based on the heterojunction between a layer of PbSe QDs and a ZnO thin film with an efficiency of 1.6% were reported.[143] The authors believe that the operation of this type of cells is similar to that of exciton solar cells (V_{oc} is determined by the energy difference between the bottom of the conduction band of ZnO and the top of the valence band of PbSe) rather than based on the p–n-junction.

Cells with a heterojunction between PbSe QDs and ZnO nanocrystals were also studied.[35] The most efficient devices were characterized by $V_{oc} = 0.44$ V, $J_{sc} = 24$ mA cm^{-2}, FF = 0.32 and $\eta = 3.4\%$. As the QD increases (E_g decreases), V_{oc} decreases and vanishes at a QD size corresponding to such mutual position of energy levels at which electron transfer from PbSe to ZnO is impossible. It was also stated that no p–n-junction is formed in the ITO/PEDOT : PSS/PbSe QDs/ZnO nanocrystals/Al structures and their operation is also similar to that of exciton solar cells.

Different principles of operation of solar cells with identical architectures can be a consequence of doping of QD layers. No formation of p–n-junctions was obtained in the studies [35, 143] where PbSe QDs treated with ethanedithiol were used. However, it was shown that treatment of PbS QDs with ethanedithiol leads to significant decrease in the concentration of majority charge carriers; this explains the absence of p–n-junction.

An original method for fabrication of heterojunctions was proposed.[144] Nanocrystals (PbS) were grown by high-temperature colloidal method using organometallic precursors on a substrate covered with a TiO_2 film and placed in a reaction vessel. This gave a completely inorganic semiconductor/oxide interface; solar cells based on this heterojunction were characterized by $\eta = 1.2\%$.

Heterojunctions formed using other compositions of nanostructured semiconductors, *e.g.*, SnS nanocrystals/PbS nanocrystals,[145] CdSe nanorods/CdSe QDs,[146] PbS QDs/silicon nanoneedles [147] are also utilized. Bilayer cells based on CdTe and CdSe nanorods with an efficiency of $\sim$3% were reported.[37] Here, charge separation occurs as in exciton solar cells (owing to formation of the second-type heterojunction) because unirradiated nanostructured layers contain no free charge carriers and the formation of a depletion layer is unlikely.

Solar cells based on a CdTe/CdSe QDs heterojunction had an efficiency of 3%.[148] However, the fabrication procedure of the QD film involved thermal annealing at 410 °C; therefore, the films exhibited the properties of bulk material.

IX. Quantum dot-sensitized solar cells

Dye-sensitized Grätzel cells are of interest because they exhibit high efficiency and are relatively cheap.[149] Owing to thorough choice of optimum sensitizers, electrolytes and anode material, the maximum efficiency of such cells known to date is about 12%.[12] The sensitizers were bipyridine ruthenium complexes whose main drawbacks are high cost and low photostability. For this type of solar cells, an investigation line is related to the use of semiconductor QDs instead of organic sensitizers (dyes).

1. The principle of operation

A schematic of a QD-sensitized solar cell is shown in Fig. 10. Quantum dots adsorbed on the surface of mesoporous TiO_2 films absorb solar radiation. Excitons produced dissociate at the QDs/TiO_2 interface. Electrons are injected into the nanoporous TiO_2 layer and transferred to anode. The initial state of QDs is recovered at the expense of electron transfer from the electrolyte. Polysulfide (S^{2-}/S_x^{2-}) (Refs 150 and 151) or cobalt (Co^{2+}/Co^{3+}) (Res. 45, 152, 153) forms of solutions of the complexes were utilized as electrolyte instead of iodide /triiodide (I^-/I_3^-) used for organic dye-sensitized solar cells because the latter compound usually promotes photoinduced corrosion of QDs.

The following reactions proceed at the QDs/polysulfide electrolyte interface:

$$S^{2-} + 2h^+ \longrightarrow S \quad (1)$$

$$S + S_{x-1}^{2-} \longrightarrow S_x^{2-} \quad (2)$$

$x = 2-5$

The electrolyte regenerates at the cathode (counter electrode)

$$S_x^{2-} + 2e^- \longrightarrow S_{x-1}^{2-} + S^{2-} \quad (3)$$

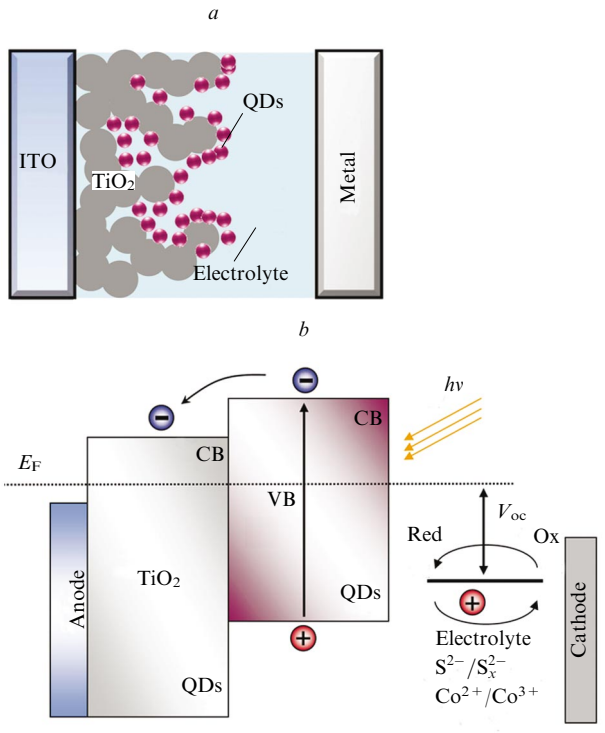


Figure 10. QD-sensitized solar cell: a schematic (*a*) and energy diagram (*b*).
CB is conduction band and VB is valence band.

The maximum open-circuit voltage in such cells is determined by the difference between the energy of the Fermi level of TiO_2 and the redox potential of the electrolyte.

A solid hole conductor, polymer P3HT, can be used instead of liquid electrolyte.[41] The active layer of the cell fabricated in Ref. 41 was composed of mesoporous titania film coated with Sb_2S_3 nanocrystals and P3HT. The Sb_2S_3 nanocrystals were chosen as a sensitizer because they are characterized by high absorption coefficient and narrow band gap. Owing to good mutual position of energy levels of the components, excitons produced upon exposure to light in both Sb_2S_3 nanocrystals and P3HT effectively dissociate at interfaces. The Sb_2S_3 nanocrystals act as electron-transport layer while the P3HT polymer acts as the hole-transport layer. Such solar cells showed high stability and good properties, *viz.*, $J_{sc} = 13.02$ mA cm^{-2}, $V_{oc} = 0.65$ V and FF = 0.61. The η was 5.13%, being among the highest results obtained for QD-sensitized solar cells.

2. Methods of fabrication

The efficiency of QD-sensitized solar cells is lower than that of organic dye-sensitized ones. This is mainly due to poor organization of QDs on the surface of titania, which is associated with inadequacy of procedures for preparation of QD layers on the surface of mesoporous films. There are two strategies of QD deposition on the anode surface.

1. Growth of QDs on the surface of a photoanode by chemical bath deposition (CBD) or by successive ionic layer adsorption and reaction (SILAR) is most often used. In the case of CBD, a photoanode is placed in a solution containing anionic and cationic precursors of nanoparticles. In SILAR, a photoanode is successively immersed in solutions of precursors. For instance, TiO_2 sensitized with CdS nanocrystals was obtained by immersion of the electrode in a solution of $Cd(NO_3)_2$ in methanol for 5 min, treatment with ethanol and subsequent drying by bubbling argon.[154] Then, the electrode was immersed in a solution of Na_2S in methanol for 5 min, washed with methanol and dried. To fabricate an efficiently operating cell, the procedure was multiply repeated.

2. The use of pre-synthesized QDs.[155, 156] An undoubtful advantage of this approach is that the morphology of the pre-synthesized nanocrystals can be controlled.

A drawback of the CBD and SILAR methods is related to difficulties in control of the size of nanocrystals; however, it is these techniques that underlie the best results obtained for sensitized solar cells. Pre-synthesized nanoparticles are covered with either a layer of original ligands or bifunctional linkers. Organic molecules separate QDs and the TiO_2 electrode; this makes electron injection less efficient. Bifunctional linkers represent molecules containing (i) carboxyl group which is attached to the surface of mesoporous oxide film and (ii) thiol group which exhibits affinity to the surface of nanocrystals. Examples of linkers are provided by thioglycolic[43, 157, 158] and mercaptopropionic[158] acids.

When using pre-synthesized particles,[159] the efficiency of a solar cell depends on the stabilizing agent on the surface of QDs. For instance, the internal quantum efficiency of cells based on n-butylamine-capped CdSe QDs is higher than that of TOPO-capped CdSe QDs due to more efficient electron transfer from QDs to TiO_2. Thioglycolic acid as a stabilizing agent provides higher rate of electron transfer and η value compared to longer-chain mercaptopropionic acid.

Quantum dots can be attached to TiO_2 surface through electrostatic interactions. For instance, the active layer composed of CdTe QDs and TiO_2 can be formed using poly(diallyldimethylammonium chloride).[160]

3. Quantum dots as sensitizers

Inorganic sensitizers for solar cells include QDs of various compositions, namely, PbS,[152, 161] CdS,[152, 162, 163] Ag_2S,[151] CdTe,[43] core–shell QDs such as CdTe@CdS,[43] PbS@CdS,[164] ZnSe@CdS,[155] CdSe,[156, 157, 165] CdTe,[156, 160] CdHgTe,[166] InP,[167] InAs[168] or Ag_2Se.[169] Different-composition QDs can also be used in the same cell. In particular, simultaneous sensitization with CdS QDs and CdSe QDs leads to better absorption of solar radiation and to an increase in I_{sc} as compared with those of devices sensitized with one type of particles.[170] At present, researchers try to use non-toxic QDs as sensitizers. Namely, solar cells based on TiS and TiO_2,[171, 172] $CuInS_2$@ZnS and ZnO[173] QDs were reported. A number of studies are devoted to the development of methods of synthesis of $(Bi_{1-x}Zn_x)S$ (Ref. 174) and $CuInS_2$ (Ref. 175) nanoparticles on TiO_2 surface.

Cells based on PbS QDs, a TiO_2 single crystal and a polysulfide electrolyte exhibited the multiple exciton generation effect.[176]

The light absorption efficiency is improved by using different-size particles.[177] For instance, the efficiency of a cell based on different-size (2.5- and 3.5-nm) CdSe QDs was

higher than those of solar cells based on same-size CdSe QDs.

Particle size /nm	2.5 and 3.5	2.5	3.5
η (%)	1.26	0.53	0.86

Also, cells based on different-size QDs are characterized by a greater extent of coverage of the photoelectrode surface and by more efficient suppression of the reverse recombination reaction between photoelectrons in the conduction band of TiO_2 and electrolyte.

Electron–hole recombination in the valence band or with a redox pair can be suppressed by doping QDs.[47] Doping with manganese led to a considerable increase in η (to 5.42%); this can be explained by the appearance of additional energy states in the bandgap. These states act as electron traps and thus preclude undesired recombination.

Organic chromophores are also used as additional sensitizers. Lee *et al.*[45] simultaneously used a ruthenium complex and QDs. His solar cells were characterized by higher efficiency than only QD-sensitized cells. Sensitization of TiO_2 was also performed with combinations of QDs and dye, *e.g.*, PbS QDs and zinc carboxyphthalocyanine; CdSv and squarylium dye.[178]

4. The photoanode

The efficiency of QD-sensitized solar cells is mainly determined by the morphology of the photoanode material. The influence of the structure of a photoanode made of TiO_2 nanoparticles on the energy conversion efficiency was studied systematically. The efficiency $\eta = 4.92\%$ was obtained for a cell with a bilayer anode whose first layer was made of 20-nm TiO_2 particles and the second layer was composed of a mixture of 20-nm and 300-nm TiO_2 particles.[42] On the one hand, utilizing large TiO_2 particles allows one to obtain a wide pore size distribution and thus a more efficient coverage of the photoanode surface with CdS/CdSe QDs, which makes pores better accessible to polysulfide electrolyte. On the other hand, scattering by large particles increases the optical path length of light and the quantum yield of the cell in the long-wavelength (> 600 nm) range.

The photoanode morphology can be improved using various 1D nanostructures, *e.g.*, TiO_2 and ZnO nanorods, nanowires and nanotubes; this favours more efficient charge separation and electron transport.[158, 179] An ITO–poly(ethylene terephthalate) flexible electrode can also be used for fabrication of solar cells.[44]

5. The choice of cathode

In the design of QD-sensitized solar cells, considerable attention is paid to the choice of metallic electrode. Polysulfide electrolyte often used in solar cells interacts with the platinum electrode, namely, S^{2-} anions are adsorbed on the electrode surface, thus suppressing conductivity and electrocatalytic activity. It was proposed to use a gold electrode instead of a platinum one. This causes the cell efficiency to increase from 3.7% to 4.22%.[170] Various carbon materials,[46, 162] Cu_2S[179, 180] including Cu_2S nanoparticles,[181] as well as CoS[182] were also proposed as cathodes.

Cells with CdS/CdSe QDs and Cu_2S as cathode showed an efficiency of 3.47%. Using ZnS[170] and SiO_2 layers,[183] the cell efficiency can be increased by suppressing recombination of excited electron at the cathode/electrolyte interface. Examples of using conductive polymers, such as polythiophene, polypyrrole, poly(3,4-ethylenedioxythiophehe)[154] for fabrication of cathode were reported. A solar cell design with no transparent electrode (ITO or FTO) was proposed; this significantly reduces the cost of the device.[179] In this case, TiO_2 nanotubes modified with CdSe QDs were synthesized on a titanium substrate. A Cu_2S ring on a brass substrate with a glass window to make the active layer accessible to light served as the cathode. The efficiency η was as high as 1.8%.

X. Conclusion

Application of QDs in solar cells is a promising and rapidly progressing research avenue in modern nanophotonics. Solar cells based on QDs are treated as third-generation photoelectric converters whose efficiency is expected to be rather high, the devices being cheaper than the first- and second-generation solar cells. Presently, there are various architectures of solar cells based on QDs. Among them, hybrid polymeric cells are best studied. However, the greatest advances were achieved in studies of semiconductor/semiconductor heterojunction cells that exhibit the highest energy conversion efficiency (6%).

Summing up, there has been considerable progress in studies on solar cells based on QDs despite a relatively short history of research efforts in the field. Significant improvement of operating parameters of cells in the nearest future is anticipated. Promising investigation lines include, first of all, the improvement of charge-carrier transport in the nanocrystalline phase to make photovoltaic devices based on QDs more efficient. Here, a key role is played by surface modification of QDs. To improve the transport properties of the nanocrystalline phase, surface ligands are replaced by shorter-chain organic molecules. However, this approach has some drawbacks related to, *e.g.*, the formation of surface traps upon replacement of ligands and to weaker adsorption of new ligands (as a consequence, oxidation of the surface of QDs becomes possible). An alternative is provided by utilizing inorganic compounds to passivate the surface of QDs. Just this approach made it possible to design cells with the maximum energy conversion efficiency among solar cells based on QDs.

The morphology of the active layer also significantly influences the efficiency. Fabrication of ordered active layers will improve charge separation and charge-carrier transport. A possible way of creating a structurally organized active layer is to use nanorod arrays (*e.g.*, titania nanorods). Also, solar cells with a cascade of different-size QD layers to ensure Förster-type energy transfer were reported.[184]

Now, various types of solar cells widely use lead chalcogenide QDs. The interest in them is due to narrow band gap and the possibility of multiple exciton generation. Studies on this effect in solar cells are available; however, a large contribution of the effect to the increase in the energy conversion efficiency has not been reported so far. Recently, the emphasis has been placed on the use of various carbon nanostructures, in particular, nanotubes and graphene, in combination with QDs in nanophotonics. Significant improvement of the properties of solar cells owing to unique electronic properties of these materials is anticipated.

This review has been written with the financial support from the Programme No. 24 of the Presidium of the Russian Academy of Sciences 'Fundamentals of Technologies of Nanostructures and Nanomaterials'.

References

1. J H Zhao, A H Wang, M A Green, F Ferrazza *Appl. Phys. Lett*. **73** 1991 (1998)
2. W Shockley, H Q Queisser *J. Appl. Phys*. **32** 510 (1961)
3. S E Shaheen, D S Ginley, G E Jabbour *MRS Bull*. **30** 10 (2005)
4. J A Renz, P A Troshin, G Gobsch, V F Razumov, H Hoppe *Phys. Status Solidi* **2** 263 (2008)
5. P A Troshin, H Hoppe, A S Peregudov, M Egginger, S Shokhovets, G Gobsch, N S Sariciftci, V F Razumov *ChemSusChem*. **4** 119 (2011)
6. D K Susarova, E A Khakina, P A Troshin, A E Goryachev, N Serdar Sariciftci, V F Razumov, D A M Egbe *J. Mater. Chem*. **21** 2356 (2011)
7. D K Susarova, P A Troshin, Y L Moskvin, S D Babenko, V F Razumov *Thin Solid Films* **519** 4132 (2011)
8. P A Troshin, D K Susarova, E A Khakina, A A Goryachev, O V Borshchev, S A Ponomarenko, V F Razumov, N Serdar Sariciftci *J. Mater. Chem*. **22** 18433 (2012)
9. L Huo, S Zhang, X Guo, F Xu, Y Li, J Hou *Angew. Chem., Int. Ed*. **50** 9697 (2011)
10. Z He, C Zhong, X Huang, W-Y Wong, H Wu, L Chen, S Su, Y Cao *Adv. Mater*. **23** 4636 (2011)
11. Z He, C Zhong, S Su, M Xu, H Wu, Y Cao *Nat. Photon*. **6** 593 (2012)
12. C-Y Chen, M Wang, J-Y Li, N Pootrakulchote, L Alibabaei, C Ngoc-le, J D Decoppet, J-H Tsai, C Gratzel, C-G Wu, S M Zakeeruddin, M Gratzel *ACS Nano* **3** 3103 (2009)
13. D V Talapin, J-S Lee, M V Kovalenko, E V Shevchenko *Chem. Rev*. **110** 389 (2010)
14. T Xu, Q Qiao *Energy Environ. Sci*. **4** 2700 (2011)
15. M Skompska *Synth. Met*. **160** 1 (2010)
16. S Ruhle, M Shalom, A Zaban *Chem. Phys. Chem*. **11** 2290 (2010)
17. A J Nozik, M C Beard, J M Luther, M Law, R J Ellingson, J C Johnson *Chem. Rev*. **110** 6873 (2010)
18. H Fu, S-W Tsang *Nanoscale* **4** 2187 (2012)
19. S Emin, S P Singh, L Han, N Satoh, A Islam *Sol. Energy* **85** 1264 (2011)
20. R Debnath, J Tang, D A Barkhouse, X Wang, A G Pattantyus-Abraham, L Brzozowski, L Levina, E H Sargent *J. Am. Chem. Soc*. **132** 5952 (2010)
21. G I Koleilat, L Levina, H Shukla, S H Myrskog, S Hinds, A G Pattantyus-Abraham, E H Sargent *ACS Nano* **2** 833 (2008)
22. H Fu, S -W Tsang, Y Zhang, J Ouyang, J Lu, K Yu, Y Tao *Chem. Mater*. **23** 1805 (2011)
23. W Ma, J M Luther, H Zheng, Y Wu, A P Alivisatos *Nano Lett*. **9** 1699 (2009)
24. J D Olson, Y W Rodriguez, L D Yang, G B Alers, S A Carter *Appl. Phys. Lett*. **96** 242103 (2010)
25. Y Zhou, M Eck, C Veit, B Zimmermann, F Rauscher, P Niyamakom, S Yilmaz, I Dumsch, S Allard, U Scherf, M Krüger *Sol. Energy Mater. Sol. Cells* **95** 1232 (2011)
26. J Seo, M J Cho, D Lee, A N Cartwright, P N Prasad *Adv. Mater*. **23** 3984 (2011)
27. K M Noone, E Strein, N C Anderson, P-T Wu, S A Jenekhe, D S Ginger *Nano Lett*. **10** 2635 (2010)
28. Y Wu, G Zhang *Nano Lett*. **10** 1628 (2010)
29. S Dayal, N Kopidakis, D C Olson, D S Ginley, G Rumbles *Nano Lett*. **10** 239 (2010)
30. I Gur, N A Fromer, C-P Chen, A G Kanaras, A P Alivisatos *Nano Lett*. **7** 409 (2007)
31. B Sun, H J Snaith, A S Dhoot, S Westenhoff, N C Greenham *J. Appl. Phys*. **97** 014914 (2005)
32. S Ren, L-Y Chang, S-K Lim, J Zhao, M Smith, N Zhao, V Bulovic, M Bawendi, S Gradecak *Nano Lett*. **11** 3998 (2011)
33. A G Pattantyus-Abraham, I J Kramer, A R Barkhouse, X Wang, G Konstantatos, R Debnath, L Levina, I Raabe, M K Nazeeruddin, M Gratzel, E H Sargent *ACS Nano* **4** 3374 (2010)
34. J M Luther, J Gao, M T Lloyd, O E Semonin, M C Beard, A J Nozik *Adv. Mater*. **22** 3704 (2010)
35. J J Choi, Y F Lim, M B Santiago-Berrios, M Oh, B R Hyun, L Sun, A C Bartnik, A Goedhart, G G Malliaras, H D Abruna, F W Wise, T Hanrath *Nano Lett*. **9** 3749 (2009)
36. D A R Barkhouse, R Debnath, I J Kramer, D Zhitomirsky, A G Pattantyus-Abraham, L Levina, L Etgar, M Gratzel, E H Sargent *Adv. Mater*. **23** 3134 (2011)
37. I Gur, N A Fromer, M L Geier, A P Alivisatos *Science* **310** 462 (2005)
38. H Liu, J Tang, I J Kramer, R Debnath, G I Koleilat, X Wang, A Fisher, R Li, L Brzozowski, L Levina, E H Sargent *Adv. Mater*. **23** 3832 (2011)
39. I J Kramer, D Zhitomirsky, J D Bass, P M Rice, T Topuria, L Krupp, S M Thon, A H Ip, R Debnath, H-C Kim, E H Sargent *Adv. Mater*. **24** 2315 (2012)
40. J Tang, K W Kemp, S Hoogland, K S Jeong, H Liu, L Levina, M Furukawa, X Wang, R Debnath, D Cha, K W Chou, A Fischer, A Amassian, J B Asbury, E H Sargent *Nat. Mater*. **10** 765 (2011)
41. J A Chang, J H Rhee, S H Im, Y H Lee, H-J Kim, S I Seok, M K Nazeeruddin, M Gratzel *Nano Lett*. **10** 2609 (2010)
42. Q Zhang, X Guo, X Huang, S Huang, D Li, Y Luo, Q Shen, T Toyoda, Q Meng *Phys. Chem. Chem. Phys*. **13** 4659 (2011)
43. X-Y Yu, B-X Lei, D-B Kuang, C-Y Su *Chem. Sci*. **2** 1396 (2011)
44. X Huang, S Huang, Q Zhang, X Guo, D Li, Y Luo, Q Shen, T Toyodab, Q Meng *Chem. Commun*. **47** 2664 (2011)
45. H J Lee, D W Chang, S-M Park, S M Zakeeruddin, M Gratzel, M K Nazeeruddin *Chem. Commun*. **46** 8788 (2010)
46. S Q Fan, B Fang, J H Kim, J J Kim, J S Yu, J Ko *Appl. Phys. Lett*. **96** 063501 (2010)
47. P K Santra, P V Kamat *J. Am. Chem.Soc*. **134** 2508 (2012)
48. S A Tovstun, V F Razumov *Khim. Vys. Energ*. **44** 224 (2010) [a]
49. C B Murray, D J Norris, M G Bawendi *J. Am. Chem. Soc*. **115** 8706 (1993)
50. A P Alivisatos *J. Phys. Chem*. **100** 13226 (1996)
51. X Peng, J Wickham, A P Alivisatos *J. Am. Chem. Soc*. **120** 5343 (1998)
52. D Yu Nikolenko, S B Brichkin, V F Razumov *Ros. Nanotekhnol*. **4** 42 (2009) [b]
53. S L Lin, N Pradhan, Y J Wang, X G Peng *Nano Lett*. **4** 2261 (2004)
54. M A Hines, P Guyot-Sionnest *J. Phys. Chem. B* **102** 3655 (1998)

55. R G Xie, X H Zhong, T Basche *Adv. Mater.* **17** 2741 (2005)
56. M Green, G Wakefield, P J Dobson *J. Mater. Chem.* **13** 1076 (2003)
57. K A Abel, J Shan, J-C Boyer, F Harris, F C J M van Veggel *Chem. Mater.* **20** 3794 (2008)
58. U Kumara, S N Sharmaa, S Singh, M Kara, V N Singh, B R Mehtac, R Kakkard *Mater. Chem. Phys.* **113** 107 (2009)
59. M A Hines, G D Scholes *Adv. Mater.* **15** 1844 (2003)
60. W W Yu, J C Falkner, B S Shih, V L Colvin *Chem. Mater.* **16** 3318 (2004)
61. J E Murphy, M C Beard, A G Norman, S P Ahrenkiel, J C Johnson, P R Yu, O I Micic, R J Ellingson, A J Nozik *J. Am. Chem. Soc.* **128** 3241 (2006)
62. M V Kovalenko, W Heiss, E V Shevchenko, J S Lee, H Schwinghammer, A P Alivisatos, D V Talapin *J. Am. Chem. Soc.* **129** 11354 (2007)
63. S G Hickey, C Waurisch, B Rellinghaus, A Eychmuller *J. Am. Chem. Soc.* **130** 14978 (2008)
64. D Battaglia, X G Peng *Nano Lett.* **2** 1027 (2002)
65. A A Guzelian, U Banin, A V Kadavanich, X Peng, A P Alivisatos *Appl. Phys. Lett.* **69** 1432 (1996)
66. M Furis, Y Sahoo, D J MacRae, F S Manciu, A N Cartwrightand, P N Prasad *J. Phys. Chem. B* **107** 11622 (2003)
67. D C Pan, L J An, Z M Sun, W Hou, Y Yang, Z Z Yang, Y F Lu *J. Am. Chem. Soc.* **130** 5620 (2008)
68. P M Allen, M G Bawendi *J. Am. Chem. Soc.* **130** 9240 (2008)
69. Y Yin, A P Alivisatos *Nature (London)* **437** 664 (2005)
70. D Yu Nikolenko, V F Razumov, S B Brichkin *Khim. Vys. Energ.* **44** 360 (2010) [a]
71. H-C Liao, C-C Lin, Y-W Chen, T-C Liu, S-Y Chen *J. Mater. Chem.* **20** 5429 (2010)
72. E Maier, T Rath, W Haas, O Werzer, R Saf, F Hofer, D Meissner, O Volobujeva, S Bereznev, E Mellikov, H Amenitsch, R Resel, G Trimmel *Sol. Energy Mater. Sol. Cells* **95** 1354 (2011)
73. J Tang, E H Sargent *Adv. Mater.* **20** 1 (2010)
74. Y Liu, M Gibbs, J Puthussery, S Gaik, R Ihly, H W Hillhouse, M Law *Nano Lett.* **10** 1960 (2010)
75. J P Clifford, G Konstantatos, K W Johnston, S Hoogland, L Levina, E H Sargent *Nat. Nanotechnol.* **4** 40 (2009)
76. J E Murphy, M C Beard, A J Nozik *J. Phys. Chem. B* **110** 25455 (2006)
77. K W Johnston, A G Pattantyus-Abraham, J P Clifford, S H Myrskog, S Hoogland, H Shukla, J D Klem, L Levina, E H Sargent *Appl. Phys. Lett.* **92** 122111 (2008)
78. D V Talapin, C B Murray *Science* **310** 86 (2005)
79. E J D Klem, H Shukla, S Hinds, D D MacNeil, L Levina, E H Sargent *Appl. Phys. Lett.* **92** 212105 (2008)
80. M V Kovalenko, M Scheele, D V Talapin *Science* **324** 1417 (2009)
81. M A Green, K Emery, Y Hishikawa, W Warta, E D Dunlop *Prog. Photovolt.: Res. Appl.* **20** 12 (2012)
82. J R Goldman, J A Prybyla *Phys. Rev. Lett.* **72** 1364 (1994)
83. U Woggon, H Giessen, F Gindele, O Wind, B Fluegel, N Peyghambarian *Phys. Rev. B: Condens. Matter* **54** 17681 (1996)
84. V I Klimov, D W McBranch, C A Leatherdale, M G Bawendi *Phys. Rev. B: Condens. Matter* **60** 13740 (1999)
85. J L Blackburn, R J Ellingson, O I Micic, A J Nozik *J. Phys. Chem. B* **107** 102 (2003)
86. A L Efros, V A Kharchenko, M Rosen *Solid State Commun.* **93** 281 (1995)
87. P Guyot-Sionnest, M Shim, C Matranga, M Hines *Phys. Rev. B: Condens. Matter* **60** R2181 (1999)
88. R Schaller, V Klimov *Phys. Rev. Lett.* **92** 186601 (2004)
89. R J Ellingson, M C Beard, J C Johnson, P Yu, O I Micic, A J Nozik, A Shabaev, A L Efros *Nano Lett.* **5** 865 (2005)
90. R D Schaller, M A Petruska, V I Klimov *Appl. Phys. Lett.* **87** 253102 (2005)
91. R D Schaller, J M Pietryga, V I Klimov *Nano Lett.* **7** 3469 (2007)
92. R D Schaller, M Sykora, J M Pietryga, V I Klimov *Nano Lett.* **6** 424 (2006)
93. O E Semonin, J M Luther, S Choi, H-Y Chen, J Gao, A J Nozik, M C Beard *Science* **334** 1530 (2011)
94. C Delerue, G Allan, J J H Pijpers, M Bonn *Phys. Rev. B: Condens. Matter* **81** 125306 (2010)
95. K W Johnston, A G Pattantyus-Abraham, J P Clifford, S H Myrskog, D D MacNeil, L Levina, E H Sargent *Appl. Phys. Lett.* **92** 151115 (2008)
96. J M Luther, M Law, M C Beard, Q Song, M O Reese, R J Ellingson, A J Nozik *Nano Lett.* **8** 3488 (2008)
97. J Tang, X Wang, L Brzozowski, D A R Barkhouse, R Debnath, L Levina, E H Sargent *Adv. Mater.* **22** 1398 (2010)
98. C-Y Kuo, M-S Su, Y-C Hsu, H-N Lin, K-H Wei *Adv. Funct. Mater.* **20** 3555 (2010)
99. C-Y Liu, U R Kortshagen *Nanoscale Res. Lett.* **5** 1253 (2010)
100. G Yu, J Gao, J C Hummelen, F Wudl, A J Heeger *Science* **270** 1789 (1995)
101. W U Huynh, J J Dittmer, A P Alivisatos *Science* **295** 2425 (2002)
102. W Yue, Y Zhao, S Shao, H Tian, Z Xie, Y Geng, F Wang *J. Mater. Chem.* **19** 2199 (2009)
103. M Zhu, T Cui, K Varahramyan *Microelectron. Eng.* **75** 269 (2004)
104. Y Kim, S A Choulis, J Nelson, D C Bradley *Appl. Phys. Lett.* **86** 063502 (2005)
105. J Y Kim, K Lee, N E Coates, D Moses, T-Q Nguyen, M Dante, A J Heeger *Science* **317** 222 (2007)
106. E J Meijer, D M De Leeuw, S Setayesh, E Van Veenendaa, B-H Huisman, P W M Blom, J C Hummelen, U Scherf, T M Klapwijk *Nat. Mater.* **2** 678 (2003)
107. N C Greenham, X G Peng, A P Alivisatos *Phys. Rev. B: Condens. Matter* **54** 17628 (1996)
108. X Jiang, R D Schaller, S B Lee, J M Pietryga, V I Klimov, A A Zakhidov *J. Mater. Res.* **22** 2204 (2007)
109. H Lu, D Bao, M Penchev, M Ghazinejad, V I Vullev, C S Ozkan, M Ozkan *Adv. Sci. Lett.* **3** 101 (2010)
110. Y-C Huang, W-C Yen, Y-C Liao, Y-C Yu, C-C Hsu, M-L Ho, P-T Chou, W-F Su *Appl. Phys. Lett.* **96** 123501 (2010)
111. Y-Y Lin, T-H Chu, S-S Li, C-H Chuang, C-H Chang, W-F Su, C-P Chang, M-W Chu, C-W Chen *J. Am. Chem. Soc.* **131** 3644 (2009)
112. M A Franzman, C W Schlenker, M E Thompson, R L Brutchey *J. Am. Chem. Soc.* **132** 4060 (2010)
113. S Ren, N Zhao, S C Crawford, M Tambe, V Bulovic, S Gradecak *Nano Lett.* **11** 408 (2011)
114. M Bredol, K Matras, A Szatkowski, J Sanetra, A Prodi-Schwab *Sol. Energy Mater. Sol. Cells* **93** 662 (2009)
115. F Tan, S Qu, J Wu, K Liu, S Zhou, Z Wang *Nanoscale Res. Lett.* **6** 298 (2011)
116. W J E Beek, M M Wienk, R A J Janssen *Adv. Mater.* **16** 1009 (2004)

117. C-Y Liu, Z C Holman, U R Kortshagen *Nano Lett*. **9** 449 (2009)
118. B Q Sun, E Marx, N C Greenham *Nano Lett*. **3** 961 (2003)
119. H Lee, S Kim, W-S Chung, K Kim, D Kim *Sol. Energy Mater. Sol. Cells* **95** 446 (2011)
120. Y Zhou, M Eck, C Men, F Rauscher, P Niyamakom, S Yilmaz, I Dumsch, S Allard, U Scherf, M Kruger *Sol. Energy Mater. Sol. Cells* **95** 3227 (2011)
121. Y Zhou, F S Riehle, Y Yuan, H F Schleiermacher, M Niggemann, G A Urban, M Krueger *Appl. Phys. Lett*. **96** 013304 (2010)
122. J Seo, W J Kim, S J Kim, K-S Lee, A N Cartwright, P N Prasad *Appl. Phys. Lett*. **94** 133302 (2009)
123. J N de Freitas, I R Grova, L C Akcelrud, E Arici, N S Sariciftci, A F Nogueira *J. Mater. Chem*. **20** 4845 (2010)
124. W L Ma, C Y Yang, X Gong, K Lee, A J Heeger *Adv. Funct. Mater*. **15** 1617 (2005)
125. S Zhang, P W Cyr, S A McDonald, G Konstantatos, E H Sargent *Appl. Phys. Lett*. **87** 233101 (2005)
126. J-F Chang, B Sun, D W Breiby, M M Nielsen, T I Solling, M Giles, I McCulloch, H Sirringhaus *Chem. Mater*. **16** 4772 (2004)
127. B Sun, N C Greenham *Phys. Chem. Chem. Phys*. **8** 3557 (2006)
128. J D Olson, G P Gray, S A Carter *Sol. Energy Mater. Sol. Cells* **93** 519 (2009)
129. I Lokteva, N Radychev, F Witt, H Borchert, J Parisi, J Kolny-Olesiak *J. Phys. Chem. C* **114** 12784 (2010)
130. J Liu, T Tanaka, K Sivula, A P Alivisatos, J M J Frechet *J. Am. Chem. Soc*. **126** 6550 (2004)
131. K Palaniappan, J W Murphy, N Khanam, J Horvath, H Alshareef, M Quevedo-Lopez, M C Biewer, S Y Park, M J Kim, B E Gnade, M C Stefan *Macromolecules* **42** 3845 (2009)
132. Z Lin *Chem. – Eur. J*. **14** 6294 (2008)
133. J De Girolamo, P Reiss, A Pron *J. Phys. Chem. C* **111** 14681 (2007)
134. C Querner, P Reiss, J Bleuse, A Pron *J. Am. Chem. Soc*. **126** 11574 (2004)
135. Q Zhang, T P Russell, T Emrick *Chem. Mater*. **19** 3712 (2007)
136. J Xu, J W Wang, M Mitchell, P Mukherjee, M Jeffries-El, J W Petrich, Z Lin *J. Am. Chem. Soc*. **129** 12828 (2007)
137. D Wang, J K Baral, H Zhao, B A Gonfa, V-V Truong, M A EKhakani, R Izquierd, D Ma *Adv. Funct. Mater*. **20** 1 (2011)
138. L Qian, J Yang, R Zhou, A Tang, Y Zheng, T-K Tseng, D Bera, J Xue, P H Holloway *J. Mater. Chem*. **21** 3814 (2011)
139. F S Shao, F Liu, Z Xie, L Wang *J. Phys. Chem. C* **114** 9161 (2010)
140. X Jiang, F Chen, W Qiub, Q Yan, Y Nan, H Xu, L Yang, H Chen *Sol. Energy Mater. Sol. Cells* **94** 2223 (2010)
141. J Gao, J M Luther, O E Semonin, R J Ellingson, A J Nozik, M C Beard *Nano Lett*. **11** 1002 (2011)
142. R Debnath, M T Greiner, I J Kramer, A Fischer, J Tang, D A R Barkhouse, X Wang, L Levina, Z-H Lu, E H Sargent *Appl. Phys. Lett*. **97** 023109 (2010)
143. K S Leschkies, T J Beatty, M S Kang, D J Norris, E S Aydil *ACS Nano* **3** 3638 (2009)
144. K P Acharya, E Khon, T O'Conner, I Nemitz, A Klinkova, R S Khnayzer, P Anzenbacher, M Zamkov *ACS Nano* **5** 4953 (2011)
145. A Stavrinadis, J M Smith, C A Cattley, A G Cook, P S Grant, A A R Watt *Nanotechnology* **21** 185202 (2010)
146. Y Yu, P V Kamat, M Kuno *Adv. Funct. Mater*. **20** 1464 (2010)
147. C-Y Huang, D-Y Wang, C-H Wang, Y-T Wang, Y-T Jiang, Y-J Yang, C-C Chen, Y-F Chen *J. Phys. D: Appl. Phys*. **44** 085103 (2011)
148. T Ju, L Yang, S Carter *J. Appl. Phys*. **107** 104311 (2010)
149. B O'Regan, M Grätzel *Nature (London)* **353** 737 (1991)
150. Y-L Lee, C-H Chang *J. Power Sources* **185** 584 (2008)
151. A Tubtimtae, K-L Wu, H-Y Tung, M W Lee, G J Wang *Electrochem. Commun*. **12** 1158 (2010)
152. H J Lee, P Chen, S-J Moon, F Sauvage, K Sivula, T Bessho, D R Gamelin, P Comte, S M Zakeeruddin, S I Seok, M Grätzel, M K Nazeeruddin *Langmuir* **25** 7602 (2009)
153. H J Lee, J-H Yum, H C Leventis, S M Zakeeruddin, S A Haque, P Chen, S I Seok, M Gratzel, M K Nazeeruddin *J. Phys. Chem. C* **112** 11600 (2008)
154. M-H Yeh, C-P Lee, C-Y Chou, L-Y Lin, H-Y Wei, C-W Chu, R Vittal, K-C Ho *Electrochim. Acta* **15** 277 (2011)
155. Z Ning, H Tian, C Yuan, Y Fu, H Qin, L Sun, H Agren *Chem. Commun*. **47** 1536 (2011)
156. J Chen, J L Song, X W Sun, W Q Deng, C Y Jiang, W Lei, J H Huang, R S Liu *Appl. Phys. Lett*. **94** 153115 (2009)
157. T Lopez-Luke, A Wolcott, L-P Xu, S Chen, Z Wen, J Li, E D L Rosa, J Z Zhang *J. Phys. Chem. C* **112** 1282 (2008)
158. X W Sun, J Chen, J L Song, D W Zhao, W Q Deng, W Lei *Opt. Express* **18** 1296 (2010)
159. P Szymanski, N Fuke, A Y Koposov, V W Manner, L B Hochza, M Sykora *Chem. Commun*. **47** 6437 (2011)
160. G-Y Lan, Z Yang, Y-W Lin, Z-H Lin, H-Y Liao, H-T Chang *J. Mater. Chem*. **19** 2349 (2009)
161. W Lee, J Lee, S K Min, T Park, W Yi, S-H Han *Mater. Sci. Eng., B* **156** 48 (2009)
162. Q Zhang, Y Zhang, S Huang, X Huang, Y Luo, Q Meng, D Li *Electrochem. Commun*. **12** 327 (2010)
163. W Lee, S K Min, V Dhas, S B Ogale, S-H Han *Electrochem. Commun*. **11** 103 (2009)
164. A Braga, S Gimenez, I Concina, A Vomiero, I Mora-Sero *J. Phys. Chem. Lett*. **2** 454 (2011)
165. J H Bang, P V Kamat *ACS Nano* **3** 1467 (2009)
166. Z Yang, H-T Chang *Sol. Energy Mater. Sol. Cells* **94** 2046 (2010)
167. A Zaban, O I Micic, B A Gregg, A J Nozik *Langmuir* **14** 3153 (1998)
168. P Yu, K Zhu, A G Norman, S Ferrere, A J Frank, A J Nozik *J. Phys. Chem. B* **110** 25451 (2006)
169. A Tubtimtae, M-W Lee, G-J Wang *J. Power Sources* **196** 6603 (2011)
170. Y-L Lee, Y-S Lo *Adv. Funct. Mater*. **19** 604 (2009)
171. H Tsukigase, Y Suzuki, M-H Berger, T Sagawa, S Yoshikawa *J. Nanosci. Nanotechnol*. **11** 3215 (2011)
172. H Tsukiqase, Y Suzuki, M-H Berger, T Saqawa, S Yoshiawa *J. Nanosci. Nanotechnol*. **11** 1914 (2011)
173. K-T Kuo, D-M Liu, S-Y Chen, C-C Lin *J. Mater. Chem*. **19** 6780 (2009)
174. M-K Son, H Seo, I Shin, I-K Kim, J Choi, K Prabakar, H-J Kim *Curr. Appl. Phys*. **11** S154 (2011)
175. J Feng, J Han, X Zhao *Prog. Org. Coat*. **64** 268 (2009)
176. J B Sambur, T Novet, B A Parkinson *Science* **330** 63 (2010)
177. J Chen, W Lei, W Q Deng *Nanoscale* **3** 674 (2011)
178. H J Lee, H C Leventis, S-J Moon, P Chen, S Ito, S A Haque, T Torres, F Nuesch, T Geiger, S M Zakeeruddin, M Gratzel, M K Nazeeruddin *Adv. Funct. Mater*. **19** 2735 (2009)
179. Q Shen, A Yamada, S Tamura, T Toyoda *Appl. Phys. Lett*. **97** 123107-1 (2010)

180. S Giménez, I Mora-Seru, L Macor, N Guijarro, T Lana-Villarreal, R Gumez, L J Diguna, Q Shen, T Toyoda, J Bisquert *Nanotechnology* **20** 295204 (2009)
181. M Deng, Q Zhang, S Huang, D Li, Y Luo, Q Shen, T Toyoda, Q Meng *Nanoscale Res. Lett.* **5** 986 (2010)
182. Z Yang, C-Y Chen, C-W Liu, H-T Chang *Chem. Commun.* **46** 5485 (2010)
183. Z Liu, M Miyauchi, Y Uemura, Y Cui, K Hara, Z Zhao, K Sunahara, A Furube *Appl. Phys. Lett.* **96** 233107 (2010)
184. A Ruland, C Schulz-Drost, V Sgobba, D M Guldi *Adv. Mater.* **23** 4573 (2011)

[a] — *High Energ. Chem. (Engl. Transl.)*
[b] — *Nanotechnol. Russ. (Engl. Transl.)*